Report No. BMI-1265
UC-37 Instruments
(TID-4500, 13th Ed., Rev.)

Contract No. W-7405-eng-92

A MODIFIED PILE OSCILLATOR FOR NEUTRON CROSS-SECTION MEASUREMENTS

by

James N. Anno
Richard G. Jung
Joel W. Chastain, Jr.

May 8, 1958

BATTELLE MEMORIAL INSTITUTE
505 King Avenue
Columbus 1, Ohio

DISCLAIMER

TABLE OF CONTENTS

A MODIFIED PILE OSCILLATOR FOR NEUTRON CROSS-SECTION MEASUREMENTS

James N. Anno, Richard G. Jung, and Joel W. Chastain, Jr.

A pile oscillator has been designed, constructed, and operated at the Battelle Research Reactor. This pile oscillator cycles a specimen and a standard in the same container through an annular ion chamber located in the thermal column. This almost simultaneous oscillation of the standard and specimen eliminates errors caused by power drifts or fluctuations. The use of a continuous graphite rod for the container or carrier reduces undesirable scattering effects of the carrier.

The oscillator was calibrated using the cross section of gold foil as a standard. Effects of geometry on measured cross sections were investigated. In general, larger samples gave higher apparent cross-section values than thin foils of comparable cross sections. Most measurements to date have been made on powdered-metal samples. Values obtained at Battelle are presented and compared with values from Oak Ridge on similar samples.

At present the sensitivity of the oscillator is limited to total absorption cross sections on the order of 1 mm^2 for accurate cross-section data. The limit of the accuracy of the measurements is approximately the accuracy to which the absorption cross section of the standard sample is known. An analysis of the errors indicates that cross sections on the order of 1 mm^2 can be measured to accuracies within $\pm$ 5 per cent without further modification of the oscillator. In general, the accuracy increases as the cross section is increased.

INTRODUCTION

With the development of nuclear reactors and reactor components has come the need for information on the neutron-absorption properties of materials. The magnitude of neutron absorption by a material is characterized by its atomic density (nuclei per unit volume of the material under investigation) and its absorption cross section, which is essentially the effective target area for absorption presented by a nucleus to an incident neutron. The absorption cross section can be defined as

$$\sigma_a \equiv \frac{R}{(nv)\,N} \quad , \tag{1}$$

where

R = number of absorptions per unit volume per unit time

nv = neutron flux (or commonly just "flux"), where n is the neutron density and v is the neutron velocity

N = number of nuclei per unit volume of the material under investigation.

The absorption cross section of concern in this report is that for thermal nuetrons, i.e., neutrons which are in thermal equilibrium with their environment.

In reactor technology, a knowledge of the thermal-neutron-absorption cross section of materials is primarily important to considerations of (1) neutron economy of a reactor system or of a research experiment, (2) thermal-neutron shielding properties of materials, and (3) activation of materials (since thermal neutrons are predominant in producing radioactive species by transmutation). Extensive studies of the thermal-neutron-absorption cross sections of the pure elements have been under way since the development of the first nuclear reactor. More recently, compilations of the measured absorption cross sections of nearly all the natural elements and many of the individual isotopes have been made.[1] However, practical cross-section data on commercial materials which in general have significant quantities of impurities are lacking. Minute traces of elements with large absorption cross sections can "poison" an otherwise low-cross-section material. Detailed chemical and spectrographic analyses can determine the principal impurities in materials and the quantities of each, and from the available data on the cross sections of the individual elements the total absorption cross section of the material can be calculated. However, this procedure is an indirect approach to determining the property which is of concern. A direct method is to measure the actual thermal-neutron-absorption cross sections of the materials.

Several techniques have been developed to measure thermal-neutron-absorption cross sections.[2] The principal techniques are discussed briefly below:

(1) Mass-spectrometric method. Since neutron absorption by a nucleus results in the disappearance of the particular species and the formation of a new isotopic species (i.e., the process of transmutation), analysis of a material exposed to a known neutron flux by a mass spectrometer can be used to deduce the thermal-neutron-absorption cross section of the material. The method has the disadvantage of requiring large reaction rates. Consequently, it lacks sensitivity with materials of low cross section and requires a high neutron flux. However, the method has been particularly useful in measuring the cross sections of the very strong absorbers such as samarium and gadolinium.

(2) Neutron-transmission method. By measuring the attenuation in intensity of a neutron beam produced by a sample of known thickness, the total cross section (absorption plus scattering) can be determined. If an independent measurement of the scattering cross section is made, the absorption cross section can be deduced. The method is an indirect one, but has been used with success in measurements of the cross sections of fissionable materials. However, the scattered neutrons must be measured over a 4π solid angle, and the low intensities made this difficult and time consuming.

---

(1) References at end.

(3) Danger-coefficient method. Introduction of a nonfissile absorber into a reactor produces a change in the core reactivity which is proportional to the absorption cross section of the material. The change in reactivity can be determined by measuring the period of the power-level change or by noting the change in position of a calibrated control rod necessary to maintain the reactor exactly critical. This method was one of the first to be used to measure absorption cross sections, but has the disadvantages of restricted sensitivity and the possibility of reactivity changes, caused by temperature or pressure variations, masking the results. Also, the reactor must be devoted almost entirely to the one program while measurements are being taken.

(4) Pile-oscillator method. Some of the disadvantages of the danger-coefficient method were overcome in the development of the pile-oscillator technique of measuring absorption cross sections. The pile-oscillator method again uses the change in reactivity to measure the cross section. In addition, the method utilizes the fact that a cyclic perturbation of the core reactivity produces an oscillating component of the core neutron flux whose amplitude is directly proportional to the neutron absorption cross section of the material.[3] Good statistics on the experimental data are obtained by the repeated amplitude determinations. However, this method also has the disadvantage of almost monopolizing the reactor during its use for cross-section measurements.

(5) Modified pile-oscillator technique. By placing the oscillator in a high-neutron-flux region of the reactor remote from the core, the effect of the oscillating absorber on the pile reactivity becomes negligible. However, the amplitude of the local depression in neutron flux caused by the absorber is still proportional to its neutron-absorption cross section, neglecting scattering effects. A neutron detector placed near the oscillating sample can be used to detect the local flux variation. The obvious choice of location of the apparatus is in a region such as a thermal column where thermal neutrons are predominant. If the ratio of thermal to resonance neutrons is sufficiently large, no correction is necessary for resonance-neutron-absorption by the samples. With the oscillator removed from the core, as in a thermal column, it may more properly be called a flux oscillator. However, by usage, the device is still termed either a pile oscillator or modified pile oscillator.

The first modified pile oscillator was developed at the X-10 graphite reactor at the Oak Ridge National Laboratory (ORNL).[4] Since the development of this instrument several similar devices have been constructed at other reactor facilities. This report describes the design and construction of a modified pile oscillator at the Battelle Research Reactor and measurements which have been made with this facility. This device, similar to the ORNL oscillator, cycles a material whose cross section is being measured through an annular neutron-sensitive ion chamber imbedded in the thermal column of the reactor. The amplitude of the signal from the ion chamber generated by

neutron absorption in the sample while passing through the chamber is indicative of the thermal-neutron-absorption cross section. Direct comparison of this amplitude with the amplitude of a signal generated by a standard of known cross section determines the thermal-neutron-absorption cross section of the unknown sample.

DESCRIPTION OF APPARATUS

The pile oscillator consists of a mechanical device to oscillate the sample, a neutron-sensitive ionization chamber, and an electronic system. The electronic system amplifies the voltage pulses generated within the chamber by the absorbing sample and converts the amplified pulses into easily measured units. Thermal neutrons are supplied by the thermal column of the Battelle Research Reactor. The pile oscillator and associated instruments are shown in the photograph in Figure 1.

A 1/4-hp motor drives a continuous chain, one link of which is rigidly fastened to a cam follower. The cam follower is free to move up and down between two hardened steel bars attached to a block which slides back and forth on two steel guide bars. Except at the endpoints, the cam-follower arrangement provides a constant-velocity stroke. A 5/8-in.-OD magnesium-alloy tube which carries the sample is passed through a machined hole in the block and is fastened to the steel block of the cam follower by means of a dowel pin and a set screw. The tube slides on Teflon bearings on each side of an ionization chamber imbedded in the thermal column of the reactor and makes no physical contact with the chamber. The part of the magnesium-alloy tube which enters the thermal-column flux is filled with machined graphite to prevent entrance discontinuities and hence undesirable scattering of neutrons. Provision for placement of the sample is made by machining slots at appropriate places in the graphite. The frequency of oscillation of the sample is approximately 40 c per min and the length of the stroke is approximately 32 in. A cutaway sketch of the thermal column, shown in Figure 2, illustrates the relationship of the oscillator and ion chamber with respect to the thermal column. The oscillator rod enters the side of the thermal column through a steel-lined lead sleeve imbedded in the concrete biological shield and passes through the ion chamber imbedded in the graphite of the thermal column.

The ionization chamber in use at the present time is shown in Figure 3. The active gas volume is contained between two concentric aluminum tubes insulated by polystyrene end caps. Five inches of the inner electrode is coated externally with about 2 mg per cm^2 of boron. The ionizing gas is air at 1 atm of pressure. The chamber is shock mounted in sponge rubber to prevent microphonic pulses due to mechanical vibrations. It is buried in a graphite stringer which is removable from the thermal column. The chamber is placed coaxially to the path of the oscillating sample and the sample passes through the inner electrode. High voltage for the ionization chamber is supplied by a bank of 45-v "B" batteries. Figure 4 shows the output current of the ion chamber as a function of applied voltage. At present the chamber is being operated at an applied voltage of approximately 360 v, near the plateau of the curve.

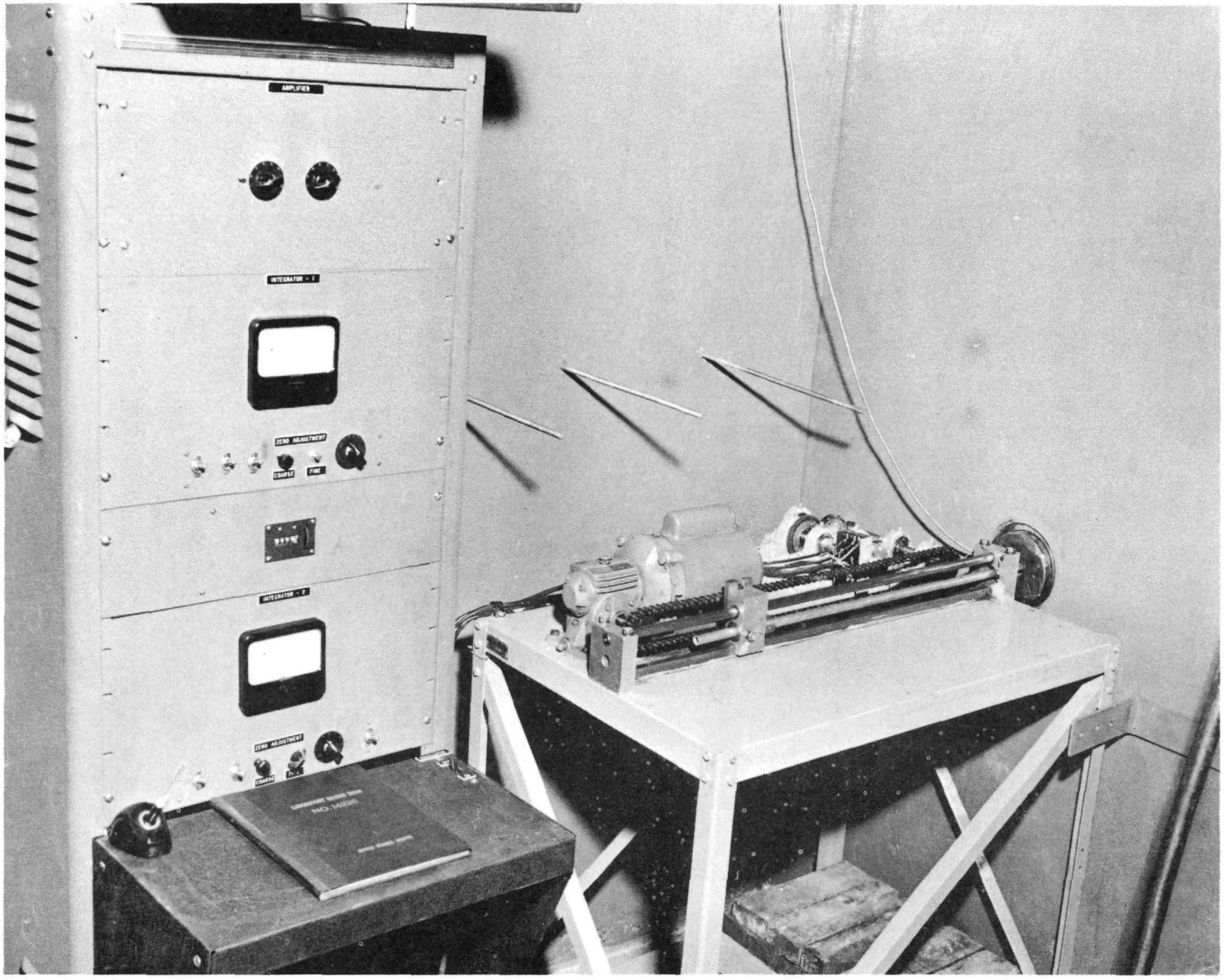

N48283

FIGURE 1. PHOTOGRAPH OF PILE OSCILLATOR FACILITY SHOWING THE OSCILLATOR MECHANISM, ACCESS TO THE THERMAL COLUMN, AND INSTRUMENT CONSOLE

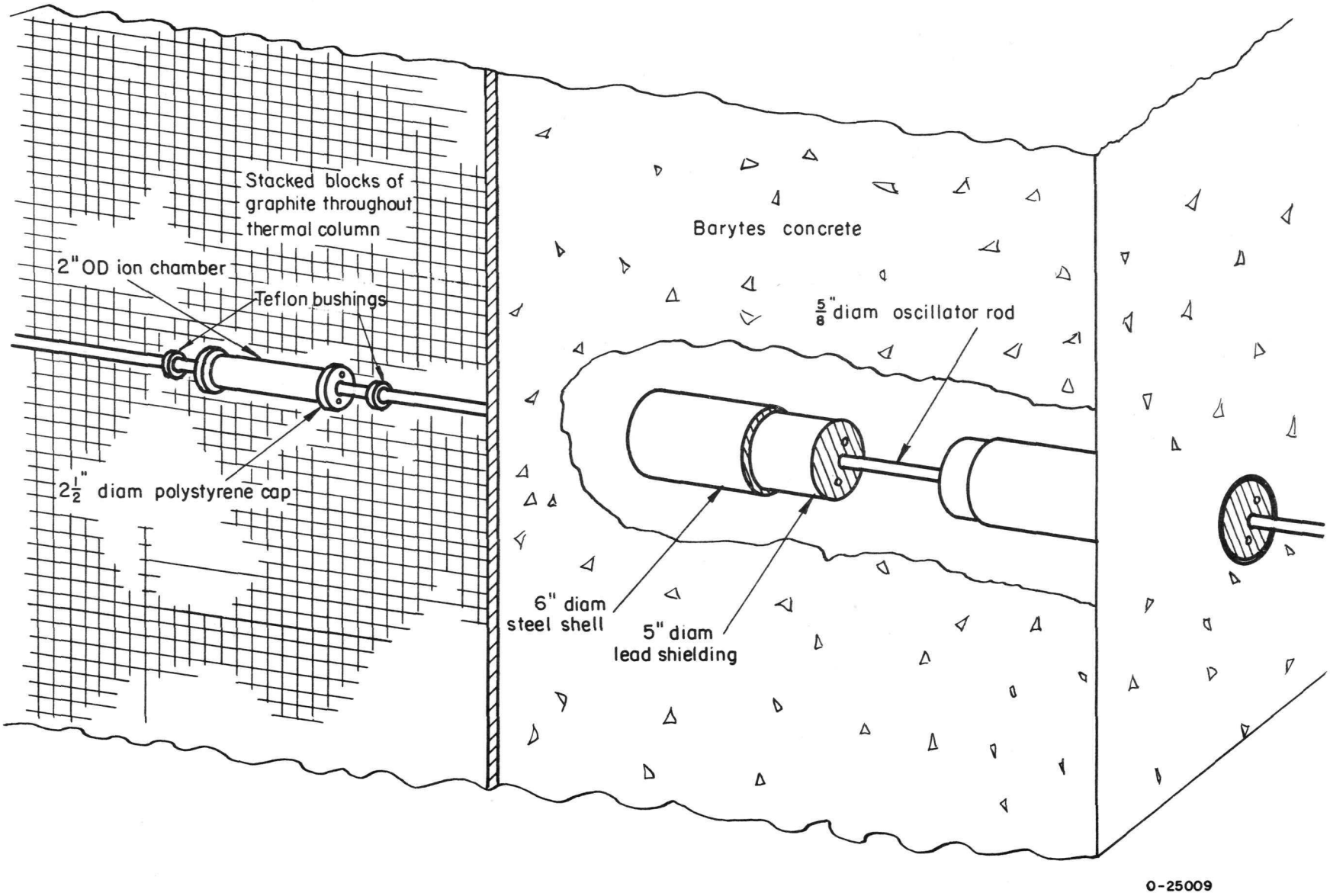

FIGURE 2. PILE-OSCILLATOR ION-CHAMBER ARRANGEMENT

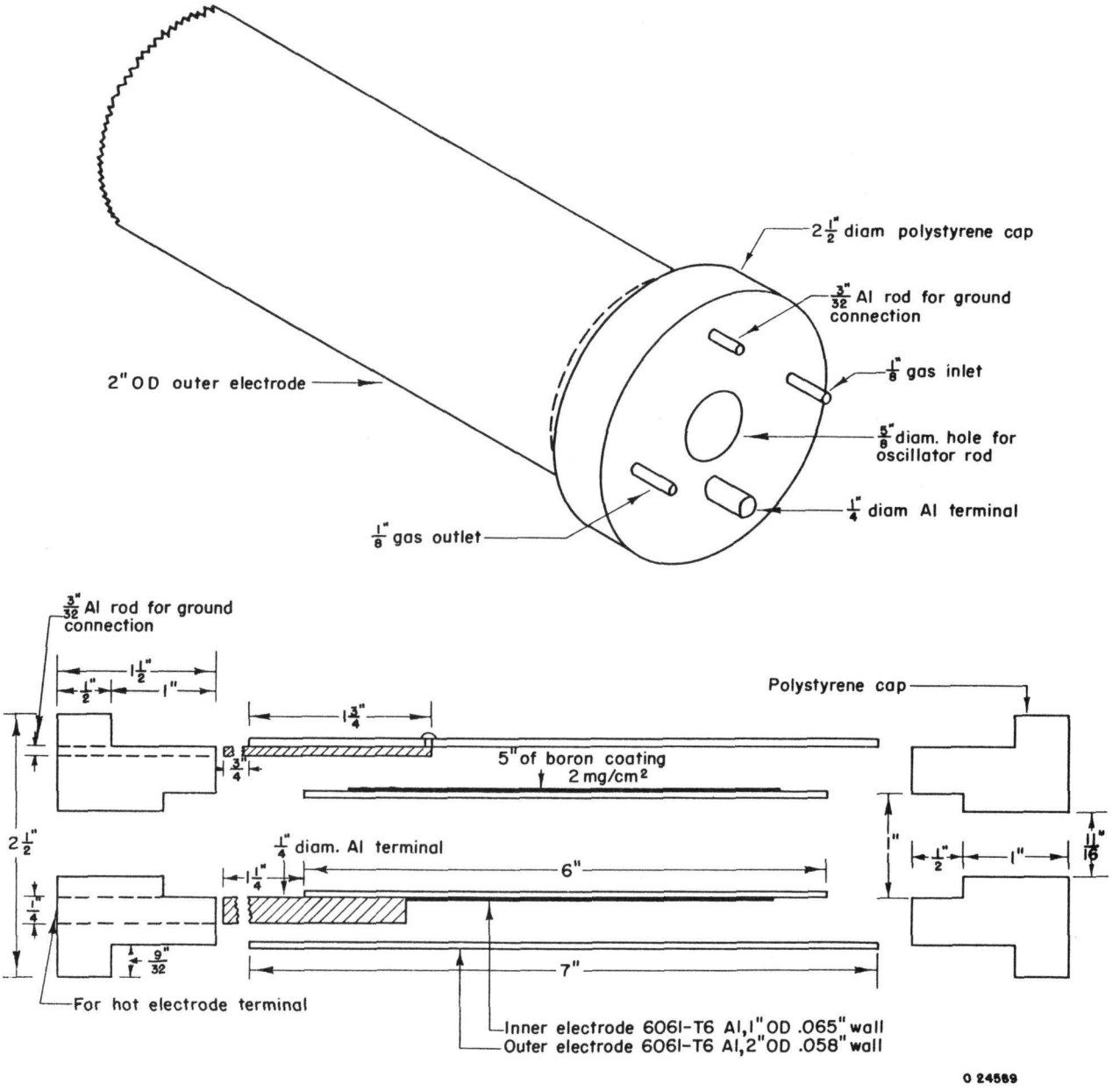

FIGURE 3. PILE-OSCILLATOR ION CHAMBER

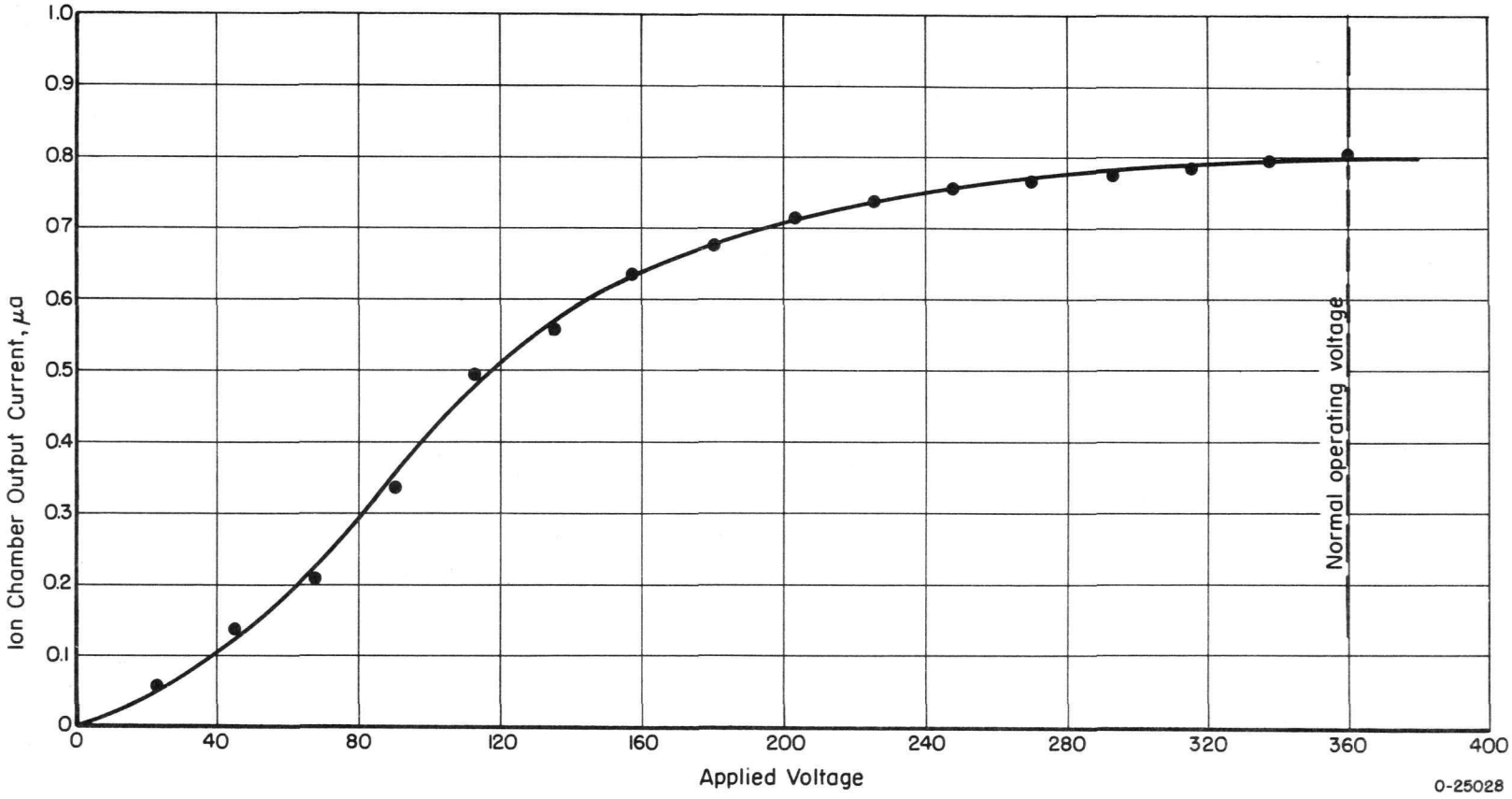

FIGURE 4. PILE-OSCILLATOR ION-CHAMBER OUTPUT CURRENT VERSUS APPLIED VOLTAGE

A block diagram of the electrical system is shown in Figure 5. The signal from the ionization chamber is amplified by a narrow-band feedback amplifier, rectified by synchronous switches, and integrated by long-time constant R-C circuits. The voltages on the integrating condensers are measured by vacuum-tube voltmeters. The B^+ voltage for the amplifier and integrators is supplied by an electronically stabilized power supply having less than 3 millivolts of ripple. The supply is of Los Alamos design. A circuit diagram is shown in Figure 6.

The amplifier and integrators are similar to those used by Hoover, et al., at Oak Ridge National Laboratory[4]. Circuit diagrams are shown in Figure 7 and Figure 8, respectively. A plot of amplification versus frequency for the amplifier on Gain 1 is shown in Figure 9. Maximum gain of the amplifier (Gain 7) is approximately five times greater. The absorption pulse from the ion chamber is at a frequency of about 4 cps so that maximum amplification of the sample signal on Gain 7 is about 30,000. One of the principal merits of the amplifier is its discrimination against high-frequency noise signals. For example, at 60 cps the amplification is only 0.05 per cent of that at 4 cps. A curve of amplifier linearity at 4 cps is shown in Figure 10. As seen from this figure, overloading begins at about a 68-v output pulse height. Thus, to avoid overloading, the total absorption cross section of the samples must be restricted to values producing output pulses of less than a 68-v amplitude.

The use of synchronous switches allows integration of the amplifier output only during that portion of the oscillator cycle during which a sample is in close proximity with the ionization chamber, thus discriminating strongly against statistical fluctuations in ion current and fluctuations in reactor power. The switches are operated by means of a gear train operated by the drive motor of the oscillator. Two switches operate the integrators and a third switch operates a Veeder-Root counter which counts the number of sample oscillations so that repeat measurements having the same number of oscillations can be made.

Two integrators are presently in use. One is used to integrate the signal from the unknown sample; the other monitors reactor power by integrating the signal from a sample of known cross section. This method continually compares the cross section of the known sample with the unknown and hence allows for correction of reactor power variations.

Of the above features of the oscillator, those considered unique to the system are the continuous graphite medium in which the samples are placed for measurement and the dual integrator system for continual calibration. Use of a continuous graphite rod eliminates axial neutron scattering due to the sample carrier, which has been observed to affect the output waveform from the ion chamber[4]. Use of the technique of continual comparison between the standard and unknown sample, in addition to correcting for reactor power drift, also minimizes errors resulting from instrument drift and from sample positioning in changing from the known to unknown sample.

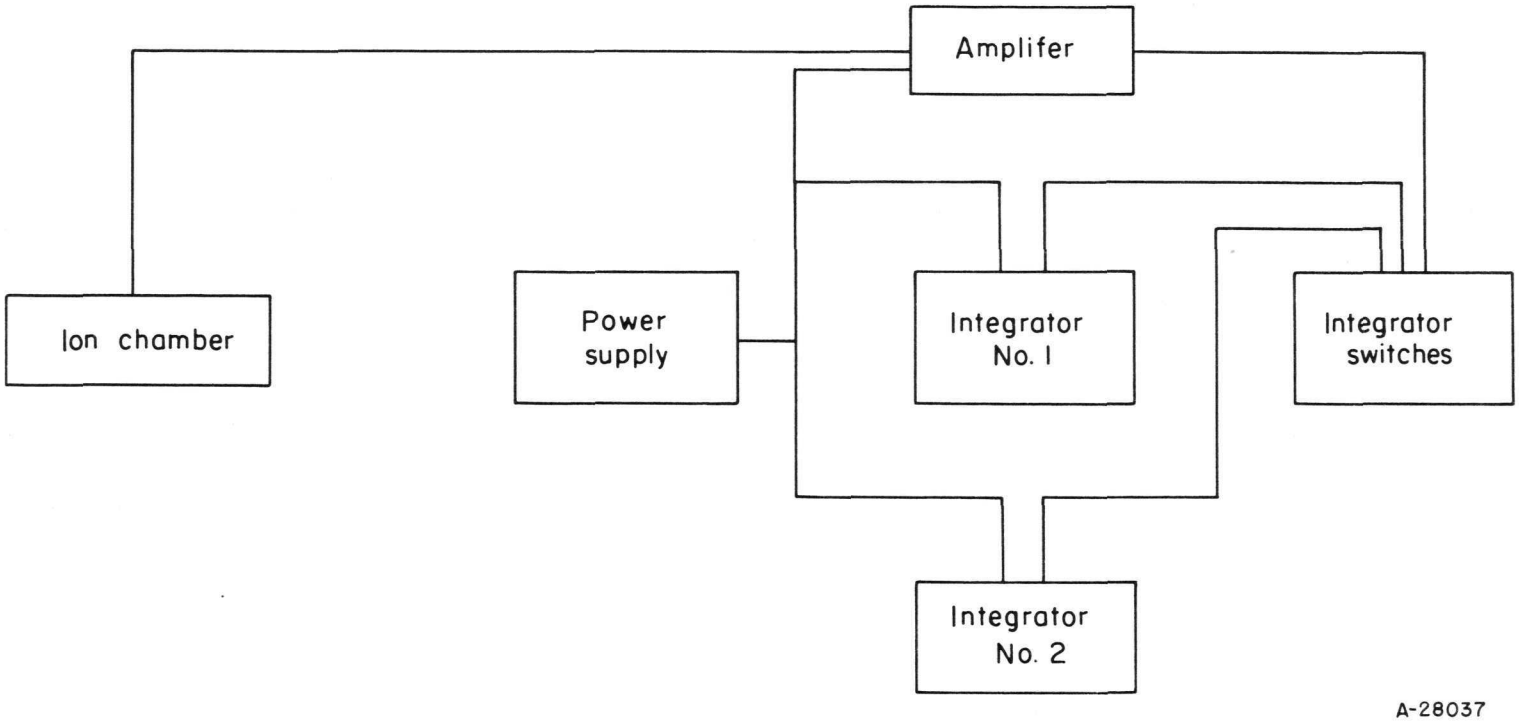

FIGURE 5. BLOCK DIAGRAM OF PILE-OSCILLATOR INSTRUMENTATION

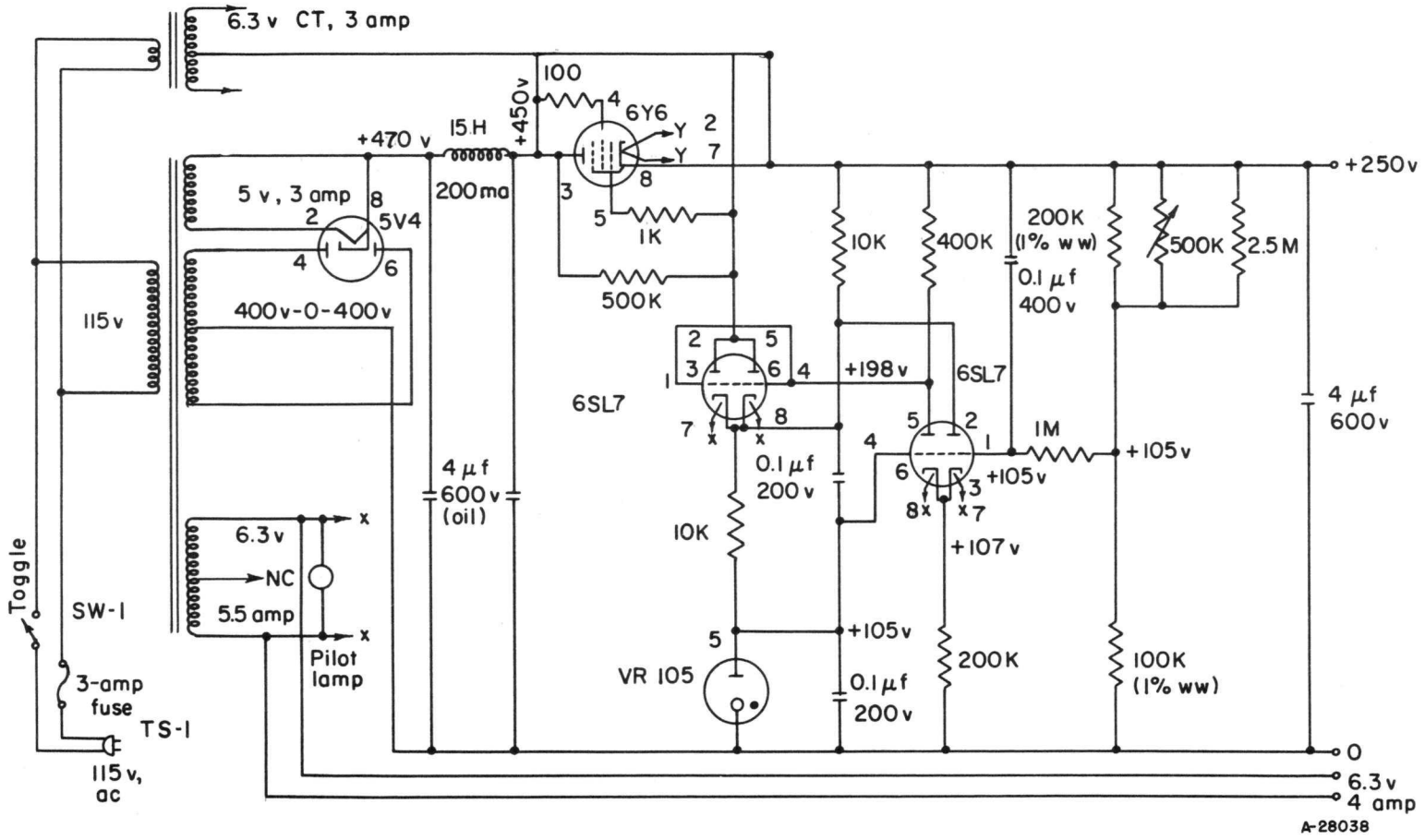

FIGURE 6. POWER SUPPLY

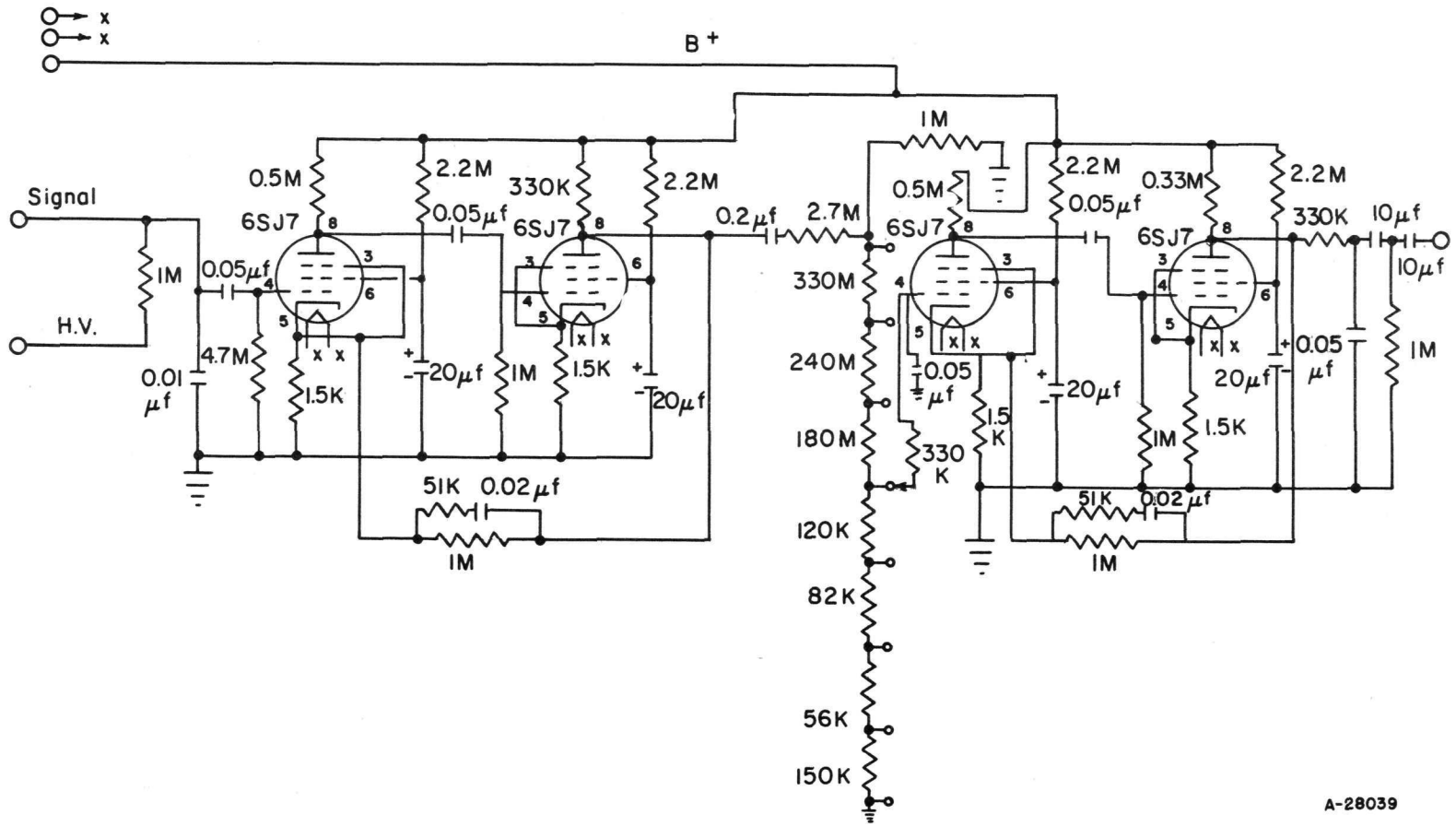

FIGURE 7. AMPLIFIER

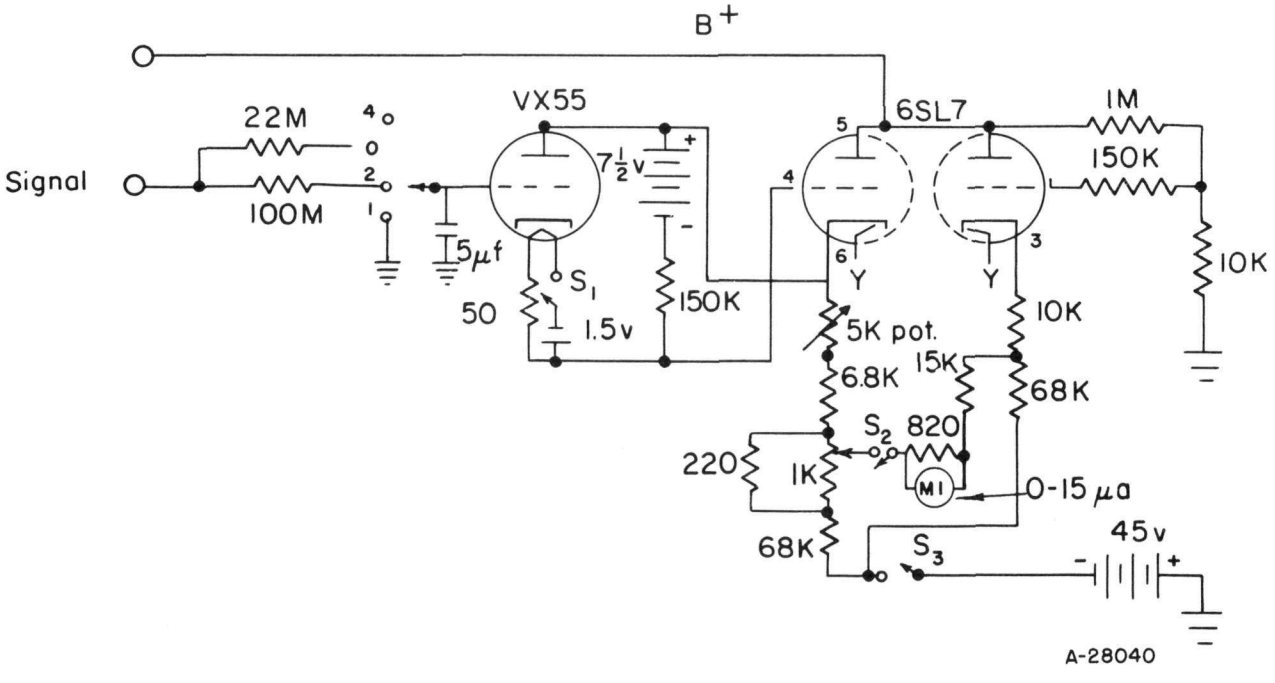

FIGURE 8. INTEGRATOR

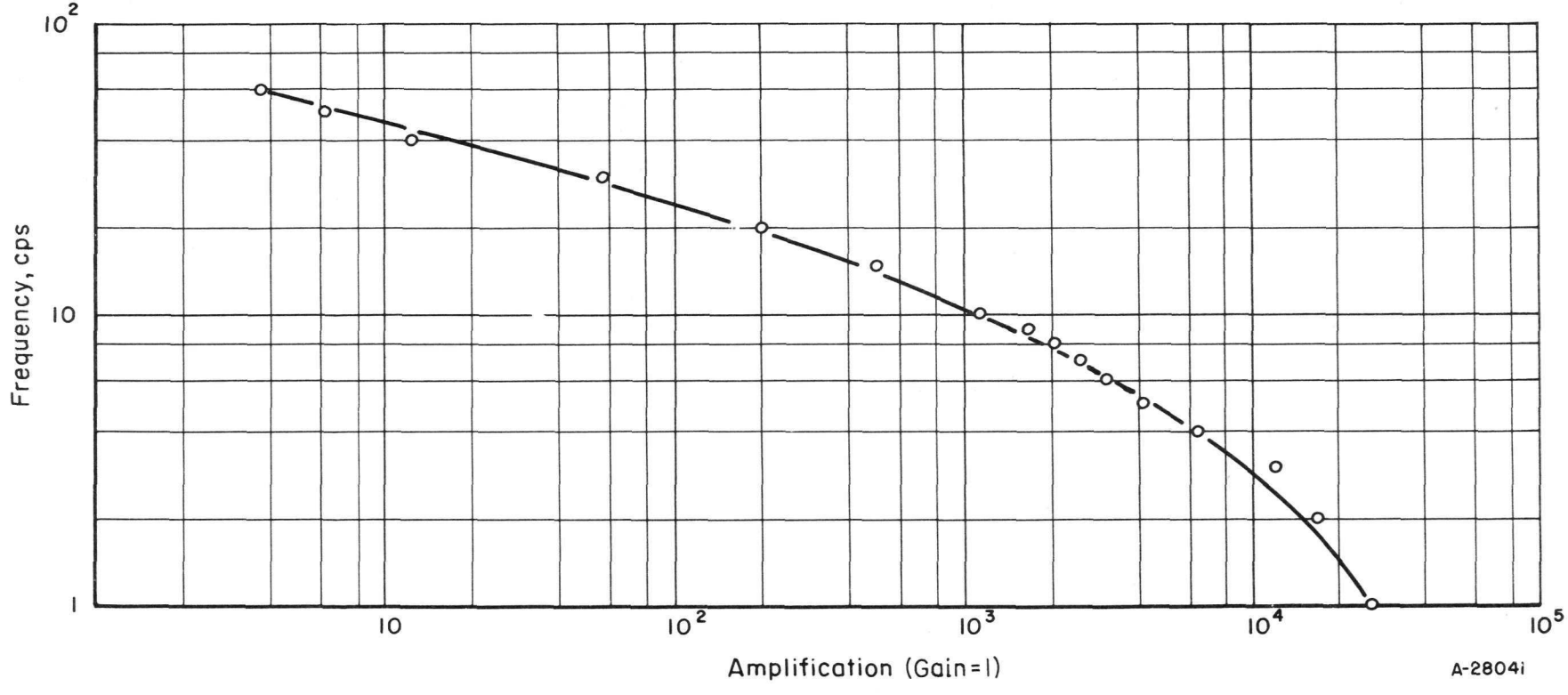

FIGURE 9. AMPLIFICATION VERSUS FREQUENCY FOR OSCILLATOR A-C AMPLIFIER

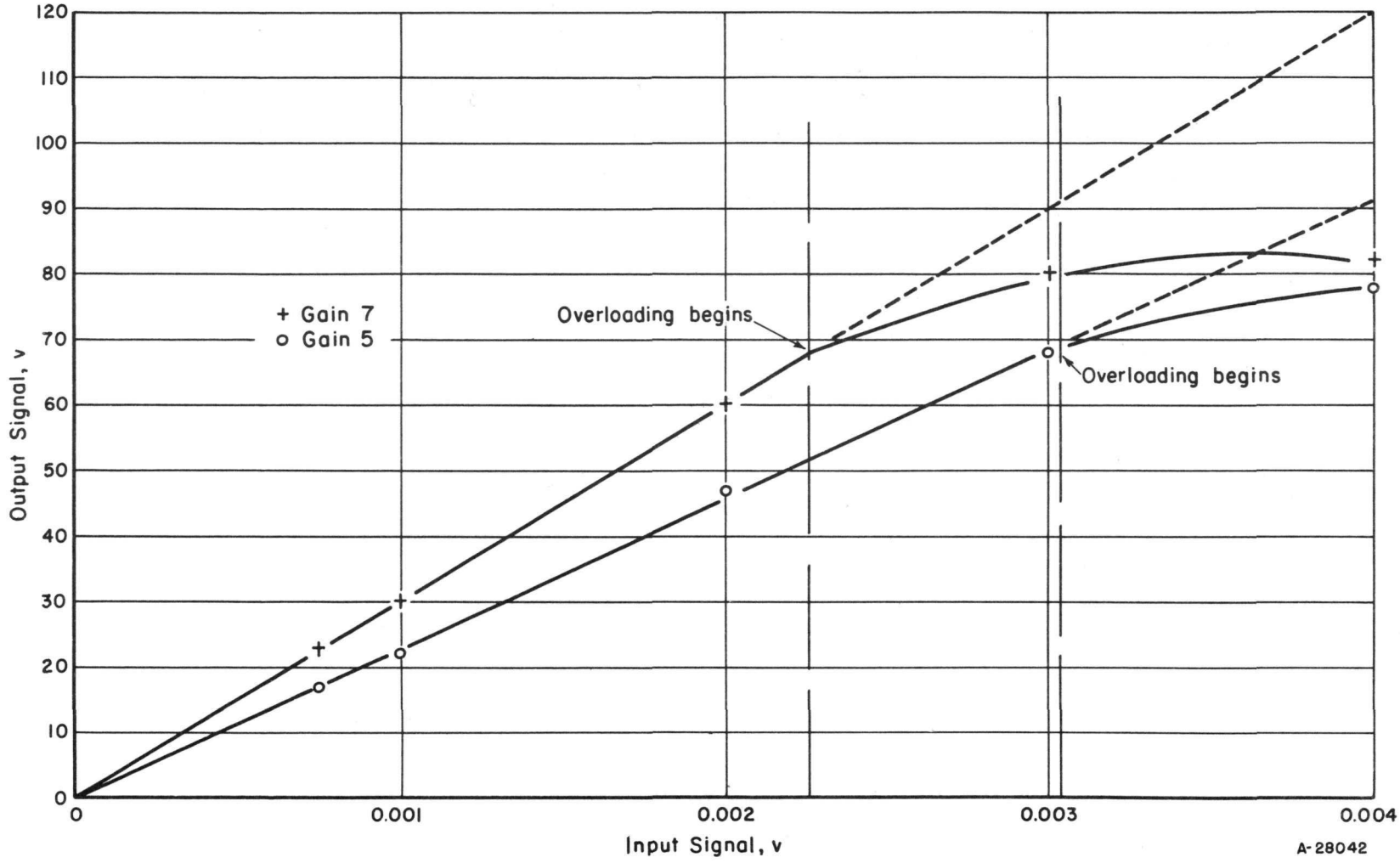

FIGURE 10. PILE-OSCILLATOR AMPLIFIER LINEARITY CURVE AT 4 CPS

NEUTRON-FLUX AND -ENERGY SPECTRUM

Since the oscillator technique is one of comparison, the magnitude of the neutron flux is not important to cross-section determinations and must only be sufficiently great to produce the desired total output current from the ion chamber. The spatial distribution of neutron flux, however, can affect cross-section measurements in its relation to neutron-scattering phenomena. Since the neutron-absorption cross section has a strong dependency on neutron energy, the energy spectrum of the neutrons absorbed by the oscillated samples must be known to properly interpret the cross-section data. For these reasons, the spatial and energy distributions of the neutron flux in the vicinity of the pile oscillator ion chamber have been measured extensively.

Thermal-Neutron-Flux Distribution

When the oscillator was first installed in the thermal column, the thermal-neutron flux at the ion chamber was below 10^8 n/(cm^2)(sec). At this time the thickness of graphite between the reactor core and the ion chamber was approximately 10 ft. This thickness of graphite, while producing a very well thermalized neutron flux (the cadmium ratio measured with 1-mil gold foils and 20-mil cadmium covers was well over 1000), attenuated the flux to such an extent that the experimental accesses to the thermal column were restricted in their usefulness to research programs. To increase the flux, the interior of the thermal column was partially voided by removal of about 25 per cent of the total graphite in the thermal column. This change reduced the effective thickness of graphite between the ion chamber and reactor core to approximately 4 ft and increased the thermal-neutron flux at the center of the ion chamber to 1.3×10^9 n/(cm^2)(sec). Reducing the graphite thickness decreased the cadmium ratio at the oscillator, but, as will be shown later in this report, the ratio of thermal to epithermal flux is still sufficiently large to eliminate most corrections on cross-section data for resonance absorption.

Since the oscillator enters the side of the thermal column (see Figure 2), most of the neutrons absorbed by the ion chamber and samples are leakage neutrons and a gradient in the spatial distribution of neutron flux exists along the axis of the ion chamber. The thermal-neutron-flux distribution along the axis is shown in Figure 11. As seen from this figure the neutron flux drop across the sensitive region of the ion chamber (the center 5 in.) is about a factor of two. This gradient can, in some cases, be important to neutron-scattering effects[5]. Positioning the ion chamber on the center line of the thermal column in the region of a flat flux distribution would eliminate scattering effects. However, as will be shown in another section of this report, for the present use of the oscillator, scattering effects are not significant. Should the need arise, with some modification, the chamber can be relocated to the region of flat flux distribution.

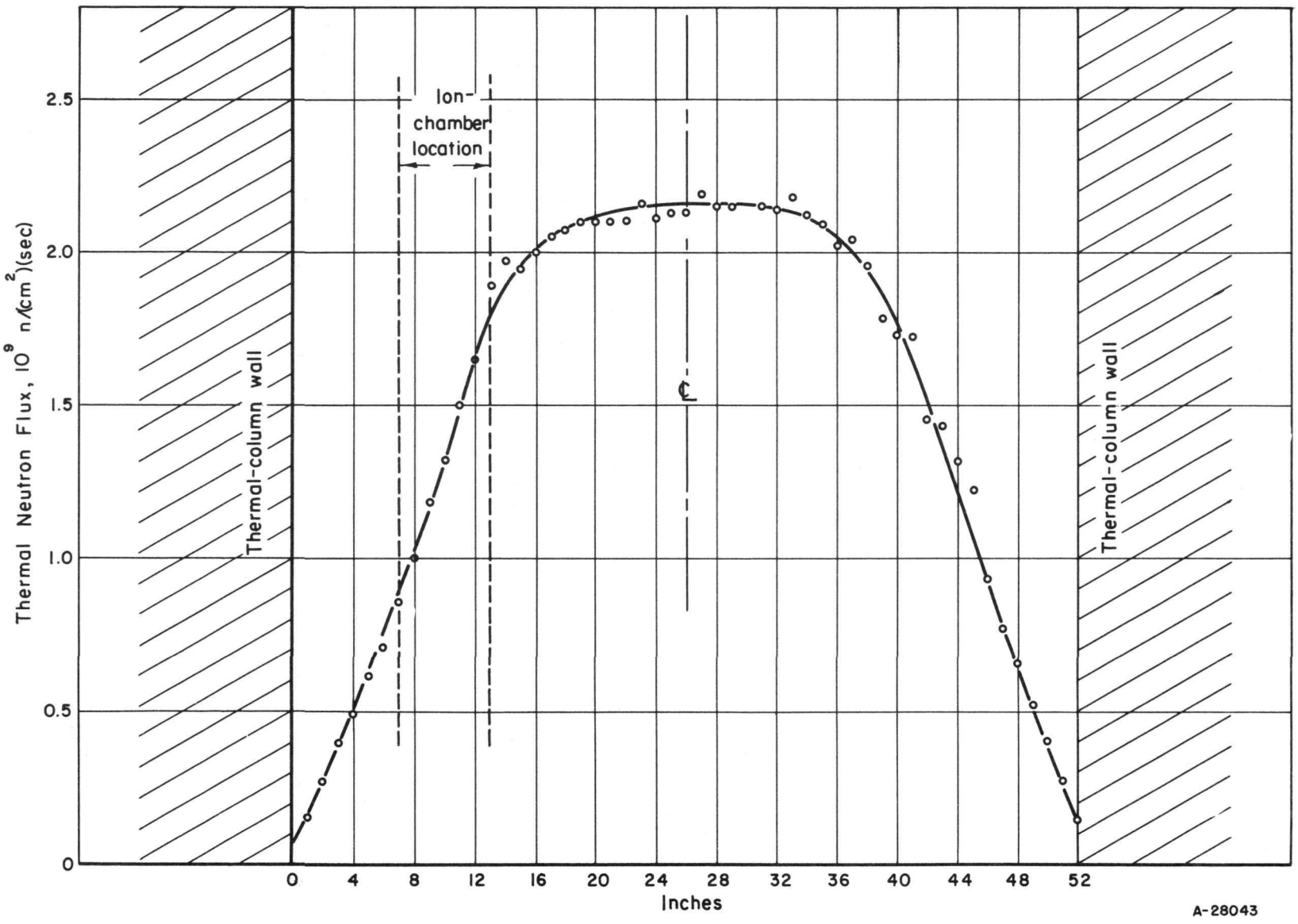

FIGURE 11. THERMAL-NEUTRON FLUX ALONG AXIS OF PILE OSCILLATOR

Thermal-Neutron Energy Spectrum

In a completely thermalized neutron flux, the energy distribution, or a parameter more readily measured – the velocity distribution – of the thermal neutrons should be Maxwellian with a distribution given by

$$dn = \frac{4n}{v_o^3 \sqrt{\pi}} v^2 e^{-\frac{v^2}{v_o^2}} dv \ , \qquad (2)$$

where

dn = number of neutrons per unit volume in the velocity range dv at the velocity v

n = total number of neutrons per unit volume

v = neutron velocity

v_o = most probable neutron velocity (2198 m per sec at 20 C).

Since most materials exhibit a 1/v absorption-cross-section dependency in the thermal-energy range, the comparison technique of the oscillator is generally valid without correction for non-1/v behavior. However, for completeness, the deviation of the thermal-neutron spectrum from the room-temperature Maxwellian distribution should be known. To obtain the velocity distribution of the neutrons at the pile oscillator, a velocity selector now under construction will be used. When samples of unknown cross-section energy dependency in the thermal-energy range are measured, the data must be qualified by stating the assumed neutron temperature so that corrections can be made as further data become available.

Epithermal-Neutron Energy Spectrum

In the graphite thermal column, the epithermal (resonance) neutrons are usually assumed to have a 1/E energy distribution. This assumption implies that the differential flux in the resonance range may be written as

$$\phi(E) = \frac{\phi_o}{E} \ , \qquad (3)$$

where

$\phi(E)$ = differential neutron flux, $n/(cm^2)(sec)(mev)$

E = energy, mev

ϕ_o = spectral constant determining the magnitude of the differential flux.

To check the assumption of a 1/E distribution, four resonance detectors with resonances in the energy range from 260 to 9100 ev were exposed in the center of the pile-oscillator ion chamber. To eliminate thermal activation of the detectors, cadmium-covered foils were used. The results are shown in Table 1.

TABLE 1. RELATIVE DIFFERENTIAL NEUTRON FLUX IN THE ENERGY REGION 260 TO 9100 EV

Reaction	Resonance Energy, ev	Cadmium Ratio	Relative Differential Neutron Flux
$Mn^{55}(n,\gamma)Mn^{56}$	260	428	8.1
$Cu^{63}(n,\gamma)Cu^{64}$	570	870	1.0
$V^{51}(n,\gamma)V^{52}$	3000	1500	0.19
$Al^{27}(n,\gamma)Al^{28}$	9100	1200	0.078

From the data in Table 1 it is seen that the cadmium ratio, defined as the ratio of the bare-foil activity to the activity of a cadmium-covered foil (20-mil-thick cadmium covers were used in this measurement), is large for all of the detectors. This indicates that the thermal neutrons are predominant in activating the foils, and, providing that the thermal-neutron-absorption cross section is similar to or less than the resonance-neutron-absorption cross section, the large cadmium ratio is indicative of a well-thermalized neutron flux. The data from Table 1 are shown graphically in Figure 12. As seen from this graph, the energy spectrum of the resonance neutrons is approximately 1/E.

Ratio of Total Thermal- to Epithermal-Neutron Flux

The ratio of the total thermal- to epithermal-neutron flux present at the oscillator ion chamber was measured by the thick-indium-foil method[6]. Briefly, this method relies upon the fact that the ratio of the thermal neutron flux to the resonance flux in any $\log_e$ energy interval can be expressed as

$$\frac{\phi_{th}}{\left(\frac{q}{\xi N \sigma_s}\right)} = \left[\frac{1}{\sigma_{th}} \int_{E_c}^{\infty} \sigma_a \frac{dE}{E}\right] \left[\frac{Q_{th}(x)}{Q_{epi}(x)}\right] \left[\frac{\frac{CR(x)}{F} - 1}{1 - X\ CR(x)}\right], \qquad (4)$$

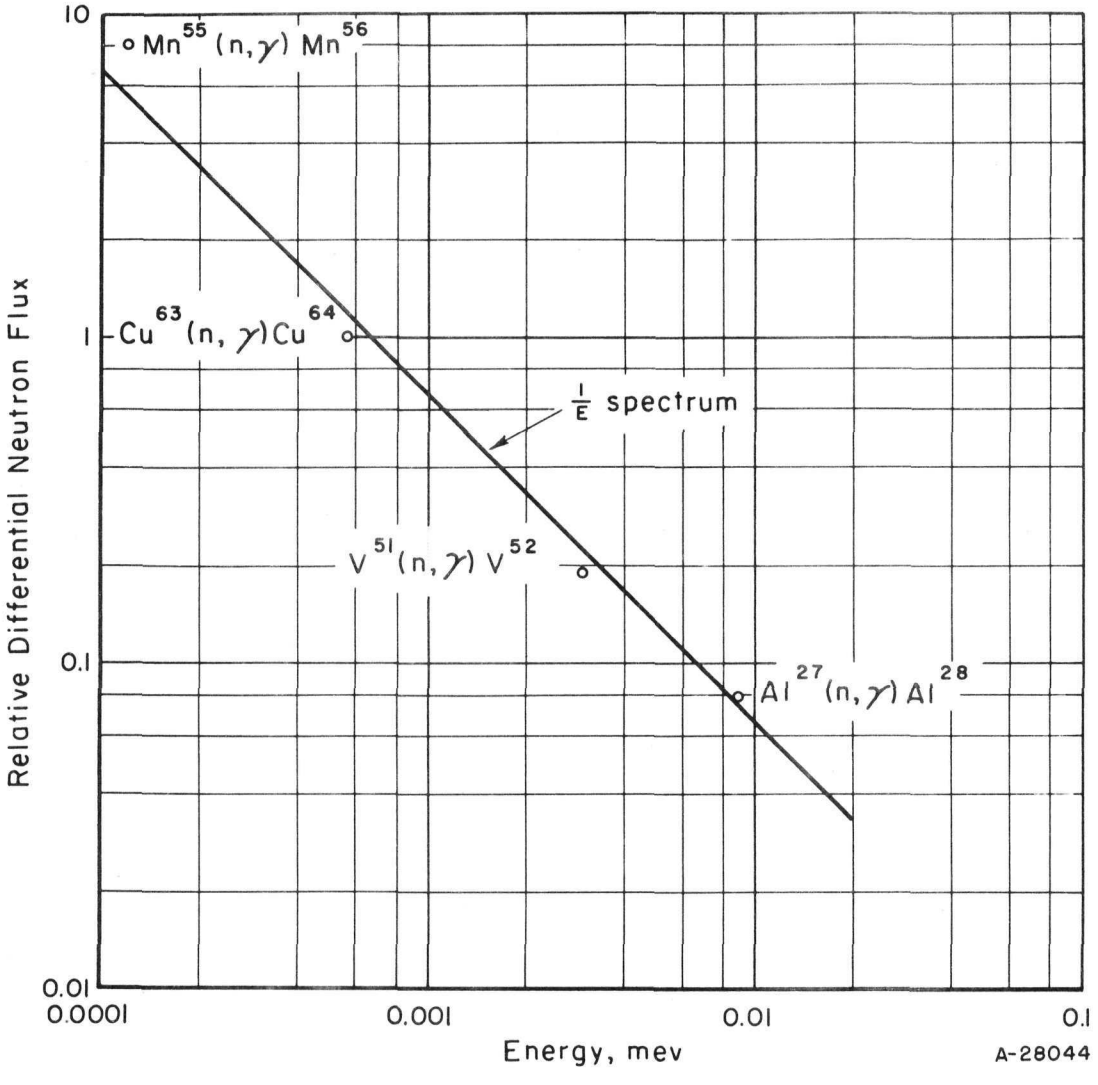

FIGURE 12. RESONANCE-NEUTRON ENERGY SPECTRUM AT PILE OSCILLATOR

where

ϕ_{th} = thermal-neutron flux

$\left(\frac{q}{\xi N\sigma_s}\right)$ = ratio of slowing down density to slowing down power = resonance flux per unit $\log_e$ energy interval

σ_{th} = thermal-neutron-absorption cross section of indium (54-min indium-116)

$\int_{E_c}^{\infty} \sigma_a \frac{dE}{E}$ = resonance absorption integral for indium (E_c = cadmium cutoff energy)

$\frac{Q_{th}(x)}{Q_{epi}(x)}$ = numerical factor depending on foil properties alone; includes effects of self-shielding, self-absorption, and self-scattering of neutrons as well as back scattering of beta particles; when x, the foil thickness, equals zero this ratio is unity

CR(x) = cadmium ratio for a particular foil thickness and cadmium cover thickness

$\frac{1}{F}$ = fraction of epithermal neutrons transmitted by the cadmium cover (a function of cover thickness)

X = fraction of thermal neutrons transmitted by the cadmium.

The cadmium ratio was found to be 1495, using indium foils of thickness approximately 40 mg per cm^2 and a 60-mil cadmium cover thickness. For this cadmium cover thickness, the value of F is about 1.24[7] and X may be assumed to be zero. The assumption that no thermal neutrons are transmitted by a 60-mil thickness of cadmium leads to a conservative estimate of the ratio $\phi_{th}/(\xi N\sigma_s)$.

To obtain the numerical value of the ratio of Equation (4), the following values of the additional parameters were used.

$$\sigma_{th} = 190 \text{ barns}$$

$$\int_{E_c}^{\infty} \sigma_a \frac{dE}{E} = 2580 \text{ barns}$$

$$\frac{Q_{th}(x)}{Q_{epi}(x)} = 0.290^{(6)}.$$

Use of these values yields a ratio of thermal flux to resonance flux in any $\log_e$ energy interval of $\frac{\phi_{th}}{(\xi N \sigma_s)} = 4750$. This information, together with the fact that the resonance-neutron energy spectrum is approximately 1/E, is sufficient to estimate errors which are involved in resonance absorption by the samples. The magnitude of the ratio of the thermal flux to total resonance flux can be estimated by assuming a resonance-neutron energy region of 0.4 ev (approximate value of cadmium cutoff energy) to 1 mev. With this energy range, the ratio of thermal flux to total resonance flux is 320, which further indicates a well-thermalized neutron flux.

WAVEFORMS AND SCATTERING EFFECTS

The waveforms of the output signals from the ion chamber have been examined. Previous studies of waveforms from other modified pile-oscillator facilities[4,8] have indicated that neutron scattering by the sample can affect the output signal. These studies also indicate that a reduction of the scattering signal may be achieved by surrounding the sample by a scattering medium such as graphite. In the apparatus described in this report, the sample is entirely surrounded by graphite. No scattering signals from samples have been observed. Physically it may be expected that some scattering effects do result, but the magnitude of the signal is apparently negligible for the present sensitivity of the system.

The signal directly from the ion chamber due to introduction of a neutron-absorbing sample is, of course, greatly amplified before being integrated. Prior to increasing the neutron flux at the oscillator by removing a portion of the graphite from the thermal column, the amplitude of the direct signal from a 1-g cadmium sample was about 0.015 v. A sketch of the signal was made from an oscilloscope trace and is shown in Figure 13. Any significant indication of scattering, which would appear as a positive signal preceding the negative absorption signal[4], was not detected. The chamber output was then connected to the amplifier and the output waveform from the amplifier observed. The resultant trace is shown in Figure 14. Another phenomenon is observed from this trace: overshoot in the amplifier is apparent, as shown by lack of immediate recovery of the signal to the base line. In order to obtain a better picture of the actual waveform, the interstage coupling time constants in the amplifier were increased by a factor of four between the first and second stages and between the third and fourth stages, and a factor of 2.5 between the second and third stages. The resulting output waveform is shown in Figure 15. This figure indicates that there was no significant scattering signal present.

Increasing the interstage time constants, although permitting a better chamber-signal reproduction, has the undesirable effect of also increasing the d-c drift in the system. During normal operation of the oscillator the interstage coupling time constants are restored to their original value and amplifier overshoot is permitted so long as recovery is made before the second oscillation or before the second sample enters the chamber if the dual integrating system is used. The integration interval is chosen to bracket the portion of the wave generated by neutron absorption rather than by the instruments.

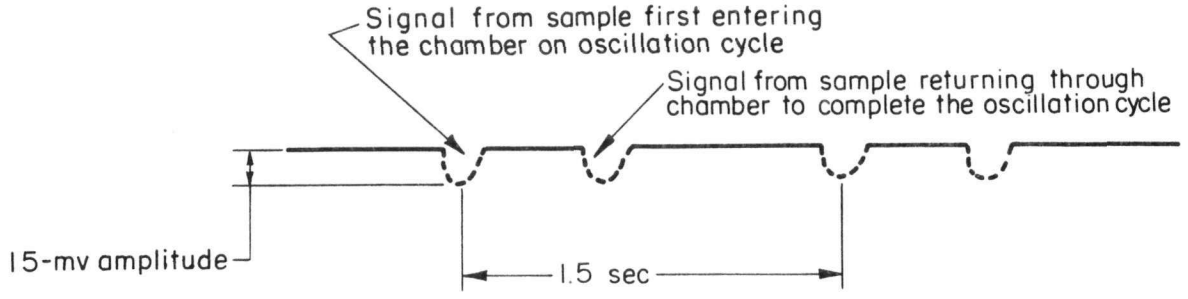

FIGURE 13. SKETCH OF SAMPLE SIGNALS DIRECTLY FROM ION CHAMBER

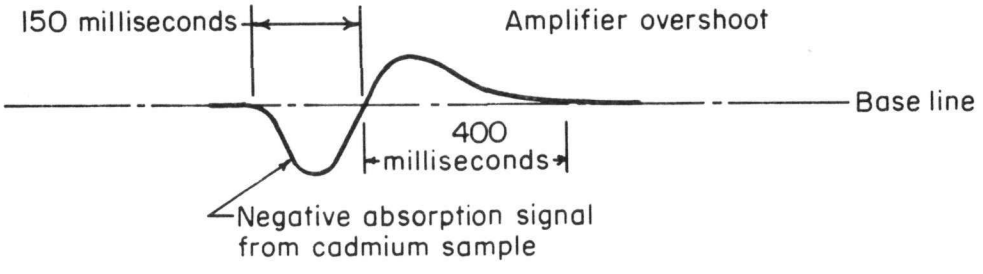

FIGURE 14. SKETCH OF WAVEFORM FROM AMPLIFIER OUTPUT

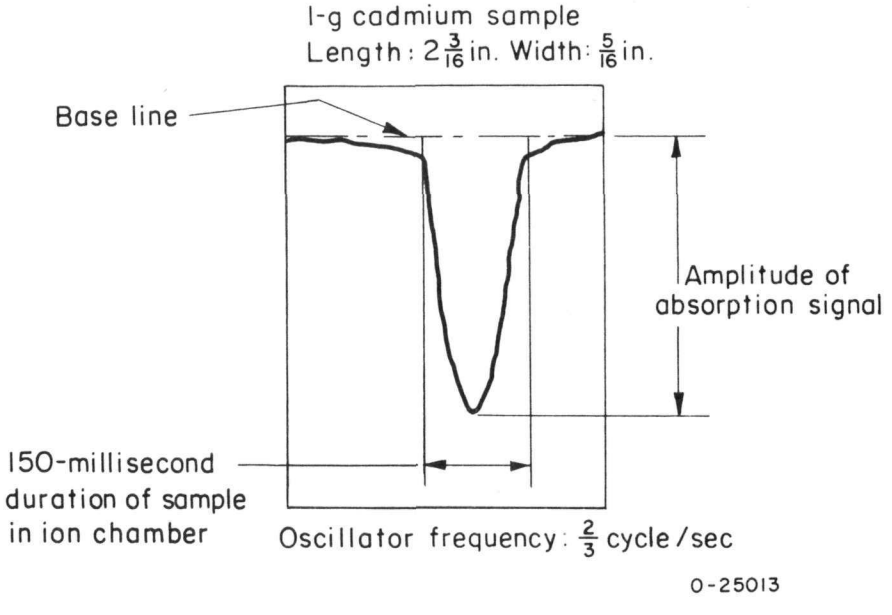

FIGURE 15. OSCILLATOR WAVEFORM DISPLAYED ON SANBORN RECORDER

Interstage coupling time constants in amplifier increased.

Cadmium, although possessing a sufficiently high absorption cross section to generate waveforms with large amplitude and hence relatively free from noise, has a very small ratio of scattering to absorption cross section. Iron, on the other hand, has a scattering cross section about five times greater than its absorption cross section. A large compressed powdered-iron sample, 2 by 5/16 by 3/16-in., was oscillated and the output waveform examined as for the cadmium. Again, no scattering signal was detected. For materials of present interest, ratios of scattering to absorption cross sections do not radically exceed that for iron. On this basis it is concluded that, for the present use of the apparatus, scattering effects are not significant.

To see if a scattering signal could be generated by removal of the continuous graphite medium in the neighborhood of the sample, the sample-carrying tube was emptied of graphite except for a 2-in. length which was left at the usual position of the absorbing sample. A scattering signal was generated and found to precede the signal due to absorption. With the tube completely filled with graphite, no signal was apparent. It was concluded that the scattering signal generated by the 2-in. graphite sample was due primarily to axial scattering of neutrons by the sample as it moved through the ion chamber.

CALIBRATION OF OSCILLATOR

Since cross-section measurements with the pile oscillator are based upon a comparison technique, the calibration of the integrator reading in terms of cross section is accomplished by observing the value for a material of known cross section and with a geometry identical to that of the sample whose cross section is to be measured. When practical, gold, with a thermal-neutron-absorption cross section of 98.0 ± 1.0 barns[1], is used as the standard for the cross-section measurements. The most convenient form of the samples is thin foil. Figure 16 shows a typical calibration curve for gold foils. The data for this curve are given in Table 2. The cross section is given in terms of mm^2 of total absorption cross section for convenience. This cross section is related to the microscopic absorption cross section as

$$\sigma\ (mm^2) = \frac{100\ M N_o \sigma_a}{A}\ , \qquad (5)$$

where

M = mass of sample, g

N_o = Avagadro's number, atoms per g-mole

A = atomic weight of sample, g per g-mole

σ_a = microscopic absorption cross section, cm^2.

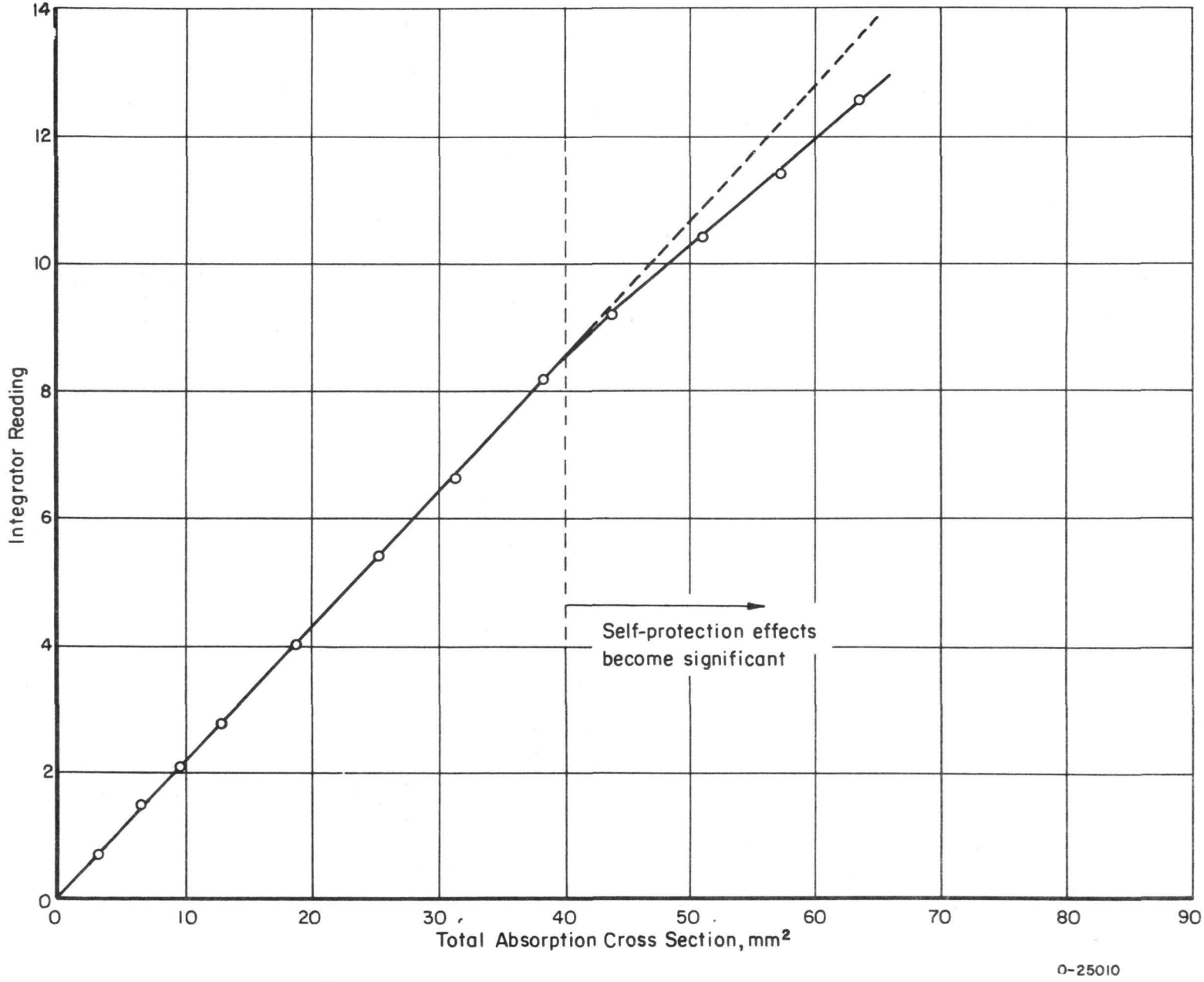

FIGURE 16. GOLD-FOIL CALIBRATION CURVE (GAIN 1)

TABLE 2. DATA FOR GOLD-FOIL CALIBRATION CURVE

Gold Foil Weight[a], mg	Total Thermal-Neutron-Absorption Cross Section, mm^2	Integrator Reading[b,c]
104	3.11	0.72 ± 0.01
214	6.40	1.50 ± 0.02
318	9.51	2.06 ± 0.01
426	12.75	2.76 ± 0.02
630	18.85	4.00 ± 0.03
842	25.2	5.46 ± 0.05
1050	31.4	6.60 ± 0.06
1277	38.2	8.16 ± 0.03
1462	43.7	9.18 ± 0.01
1708	51.1	10.40 ± 0.05
1918	57.4	11.40 ± 0.05
2126	63.6	12.54 ± 0.08

(a) Foils 2 in. long and 5/16 in. wide.
(b) Gain 1, five 1-min determinations.
(c) The probable error is given after each value.

As seen from the figure, self-protection effects (i.e., effects caused by the fact that atoms in the center of the sample see a lower neutron flux than on the edges of the sample due to absorption of neutrons in the outer regions of the sample) become significant at cross sections about 40 to 45 mm^2. The self-protection effects are present, of course, for cross sections below this amount, but are not sufficiently pronounced to cause significant deviation in the linear behavior of cross section with integrator reading.

The particular curve shown in Figure 16 was obtained for Gain 1 of the amplifier with five 1-min integrations determining each point. Each of the first five gains was similarly calibrated and the integrator reading per mm^2 of cross section for each of the gains is shown in Table 3.

TABLE 3. CALIBRATION OF INTEGRATOR FOR EACH AMPLIFIER GAIN

Amplifier Gain	Integrator Reading[a], per mm^2
1	0.152
2	0.206
3	0.298
4	0.430
5	0.621

(a) Determined from five 45-sec integrations.

Overloading of the amplifier occurs at a higher cross section than that at which self-protection effects become significant. For example, on Gain 1 the amplifier first overloads at a cross section of about 75 mm^2. The amplitude of a signal from an absorber having this cross section is about 68 v (see Figure 10) on the output of the amplifier. The overload point on the other gains, of course, occurs at increasingly lower cross sections with increasing gain.

For samples having geometry different from foils, special standards are prepared. For example, compressed powdered-metal samples have been prepared with dimensions 2 by 5/16 by 3/16 in. for cross-section measurements. For these larger samples, gold is not a suitable direct standard and secondary standards are prepared. However, as will be shown later in this report in the discussion of geometry effects, by a very special choice of dimensions of the larger samples, foils can be used to standardize the cross section.

GEOMETRY EFFECTS

The effects of sample geometry on cross-section measurements were studied by comparing cross-section data for foils, slabs, and cylinders. To obtain cross sections in the same range, three materials were used: iron cylinders, copper slabs, and gold foils. The length of all samples was 2 in. Table 4 summarizes the sample sizes and data. The integrator reading represents measurements taken in ten determinations, each of 200 oscillations. The integrator readings are plotted versus the calculated total absorption cross sections* in Figure 17. As seen from this figure, the larger the cylinders and slabs, the more the deviation from the gold-foil calibration curve. At total absorption cross sections below 15 to 20 mm^2, the integrator readings from the slabs and cylinders are less than the gold-foil readings. At cross sections greater than about 45 mm^2 (gold-foil thickness of approximately 7 mils) the effects of self-protection become apparent, i.e., the efficiency of the sample as an absorber is reduced because the center of the sample is exposed to a lower neutron flux due to neutron absorption in the outer region of the sample.

The effect of the variation of diameter of the iron cylinders on the observed cross section can better be seen from the graph of Figure 18. In this figure the integrator reading per unit of absorption cross section is plotted versus the diameter of the cylinders. As shown in this curve, as the diameter of the cylinders increases, the integrator reading per mm^2 of cross section becomes larger until self-protection effects become significant. For diameters greater than about 0.275 in. (approximately 45 mm^2 total absorption cross section), additional absorber has a diminishing effect per unit cross section. The gold-foil integrator reading per unit cross section is also shown on the graph, and is approximately constant below 45 mm^2. This would be expected since radical geometry changes are not incurred with the thin foils. It will be noted from the graph that identical integrator readings are obtained for a cylinder of 0.183-in. diameter and the gold foils. This suggests that with proper choice of sample size, geometry effects can be eliminated in comparing the cross sections of samples of widely differing geometry.

*Using the cross sections reported in BNL-325.

TABLE 4. RESULTS OF GEOMETRY STUDY WITH FOILS, SLABS, AND CYLINDERS

Sample	Thickness or Diameter, in.	Weight, g	Cross Section[a], mm^2	Integrator Reading
Iron cylinder	0.1247	3.010	8.46 ± 0.20	0.145 ± 0.011
	0.1873	7.101	19.37 ± 0.46	0.467 ± 0.027
	0.250	12.597	34.37 ± 0.81	0.934 ± 0.008
	0.312	19.634	53.6 ± 1.3	1.42 ± 0.02
	0.375	28.470	77.7 ± 1.8	1.91 ± 0.02
Copper slab, 5/16 by 2 in. by thickness	0.030	2.670	9.34 ± 0.030	0.174 ± 0.010
	0.050	4.434	15.51 ± 0.05	0.387 ± 0.014
	0.100	9.028	31.58 ± 1.03	0.846 ± 0.006
	0.1865	16.833	58.9 ± 1.9	1.47 ± 0.02
	0.250	22.666	79.3 ± 2.6	1.86 ± 0.01
Gold slab, 5/16 by 2 in. by thickness	0.00212	0.420	12.57 ± 0.13	0.297 ± 0.017
	0.00424	0.840	25.14 ± 0.26	0.618 ± 0.016
	0.00742	1.470	44.00 ± 0.45	1.05 ± 0.01
	0.0116	2.310	69.14 ± 0.71	1.54 ± 0.003

(a) Cross-section values from BNL-325.

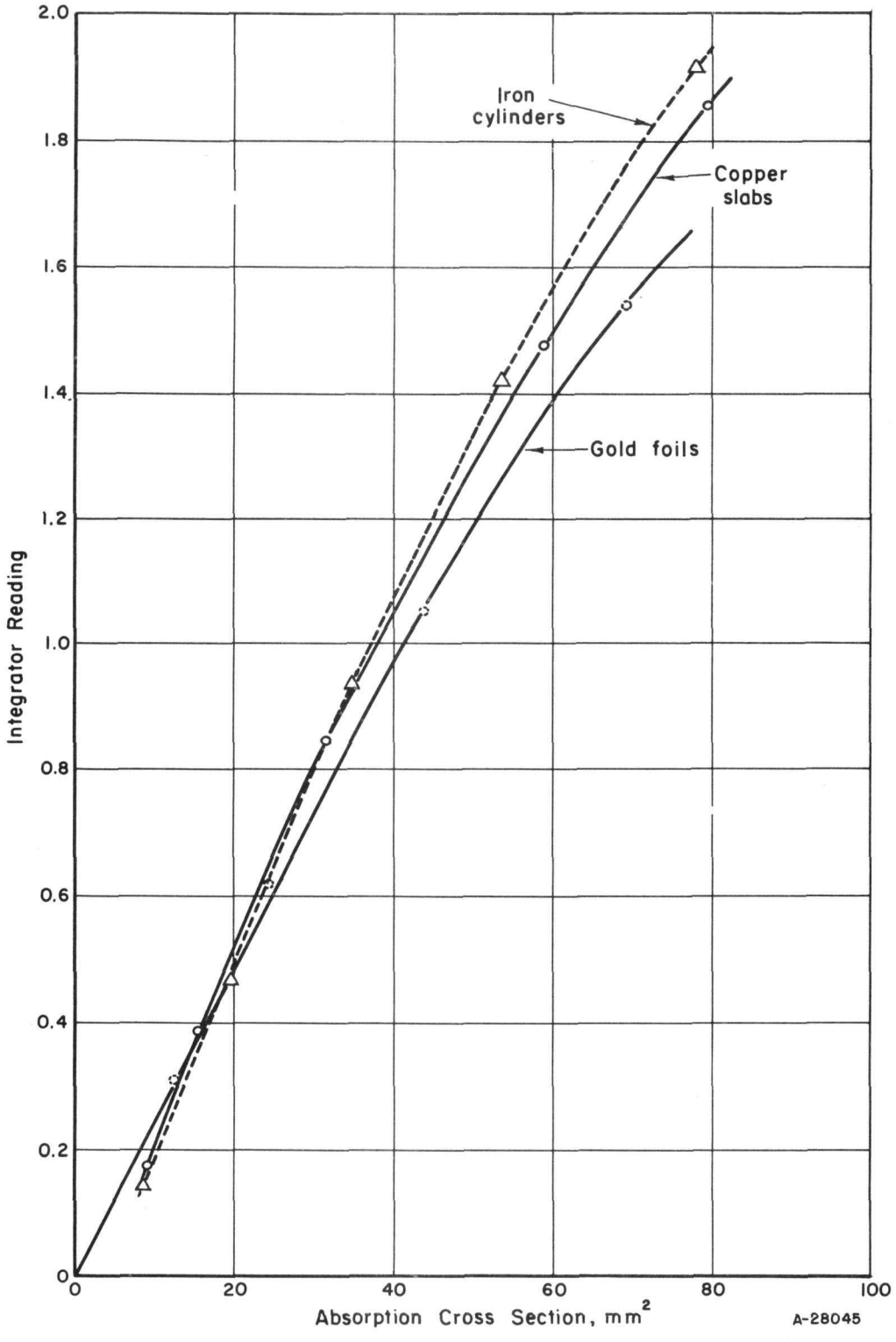

FIGURE 17. EFFECTS OF GEOMETRY ON CROSS-SECTION MEASUREMENTS

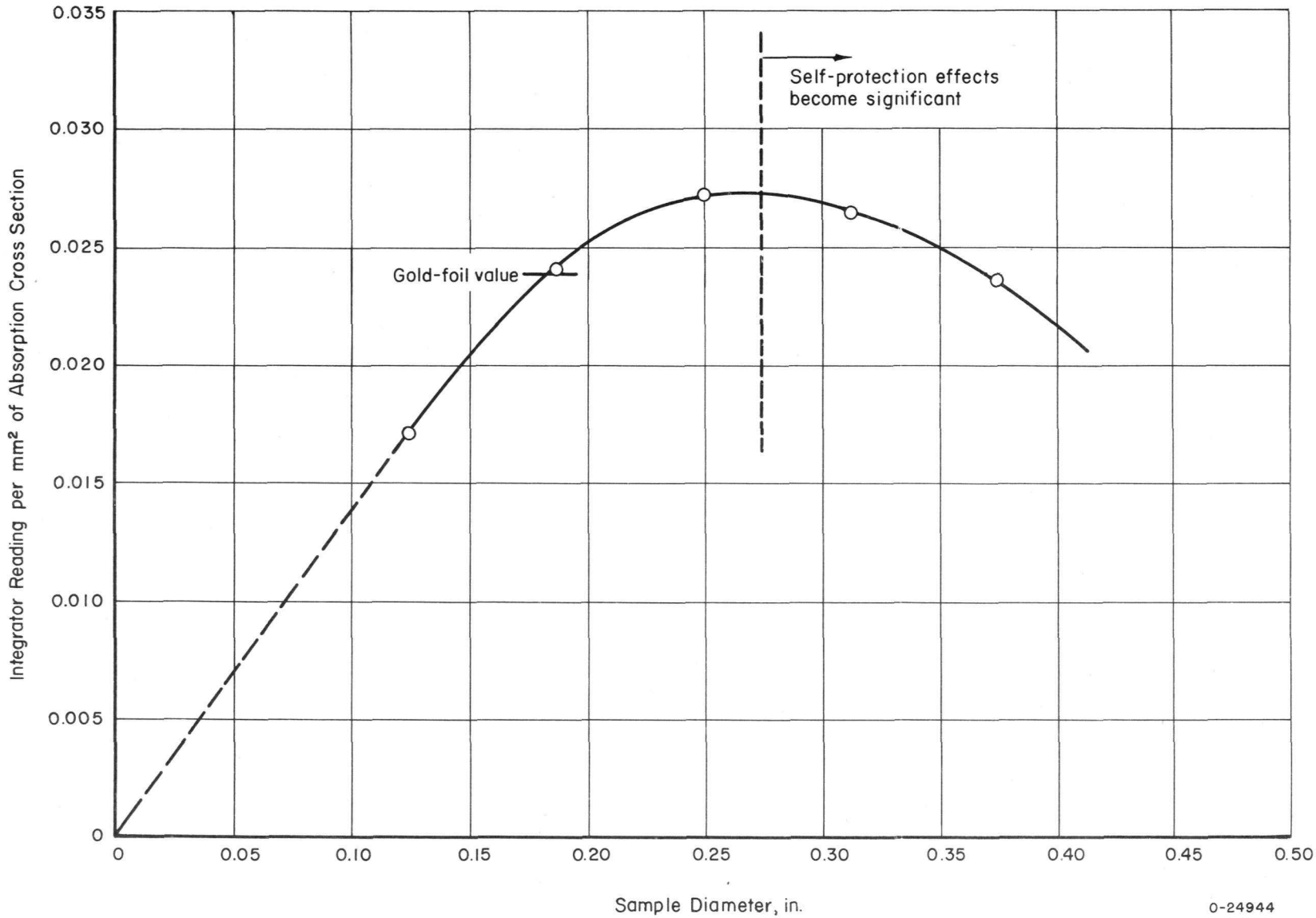

FIGURE 18. INTEGRATOR READING PER UNIT CROSS SECTION VERSUS DIAMETER OF IRON CYCLINDERS

The graph of Figure 18 represents the slope of the corresponding curve for cylinders given in Figure 17. The curve in Figure 18 appears to extrapolate reasonably well to zero, thus indicating that the curve of Figure 17 is S-shaped and approaches zero with zero slope.

It is informative to understand the reasons for the observed geometry dependence of the cross-section measurements. Because of the simplicity of geometric shape, a comparison between the iron cylinders and gold foils is most readily made in this analysis. For further simplification, a two-dimensional model is proposed. The geometry of the sample and ion chamber is shown in Figure 19.

For the cylindrical sample geometry, consider the neutrons passing through a point P on the circumference of the ion chamber. Assuming an isotropic neutron flux, a fraction $\frac{\theta}{2\pi}$ of these neutrons will be directed toward the sample. It is further assumed in this simple model that no scattering of the neutrons occur, so that a neutron once directed within the angle θ will "see" the sample. The angle θ is given in terms of the dimensions of the ion chamber and sample as

$$\theta = 2 \text{ arc sin } \left(\frac{r}{a}\right) . \tag{6}$$

Because of the symmetry of the system, for the cylinders, the angle θ for each point source around the circumference is constant.

For the foil-sample geometry given in Table 5, the angle θ' subtended by the foil from the point P' is not constant as P' (located by the angle α in Figure 19) moves around the circumference. The average angle θ'_{avg}, given by

$$\theta'_{avg} = \frac{\int_0^{2\pi} \theta'(\alpha)\, d\alpha}{\int_0^{2\pi} d\alpha} , \tag{7}$$

is found to be 0.3551 radian. Assuming that the measured cross section is proportional to this angle, then when $\theta'_{avg} = \theta$ the cross-section measurements for the foil and the cylinder with angle θ should be the same. From the experimental results, it was found that a cylinder of 0.183-in. diameter was equivalent geometrywise to the foil. This value is to be compared with the diameter of 0.179 in. at $\theta'_{avg} = \theta$ which is shown from Figure 20. Thus, simple geometric considerations predict rather well the point at which the cylinder and foil cross sections agree and indicate one of the parameters responsible for changes in the apparent cross section with geometry. For a complete analytical prediction of the geometry behavior, consideration must be given to the effective thickness of the sample, the three-dimensional characteristics, and neutron diffusion. These refinements are beyond the purposes of the present development.

Behavior similar to that of the geometry effects of the cylinders is observed for the copper slabs. At a slab thickness of 0.044 in. the integrator readings per unit cross section of the slabs and foils coincide.

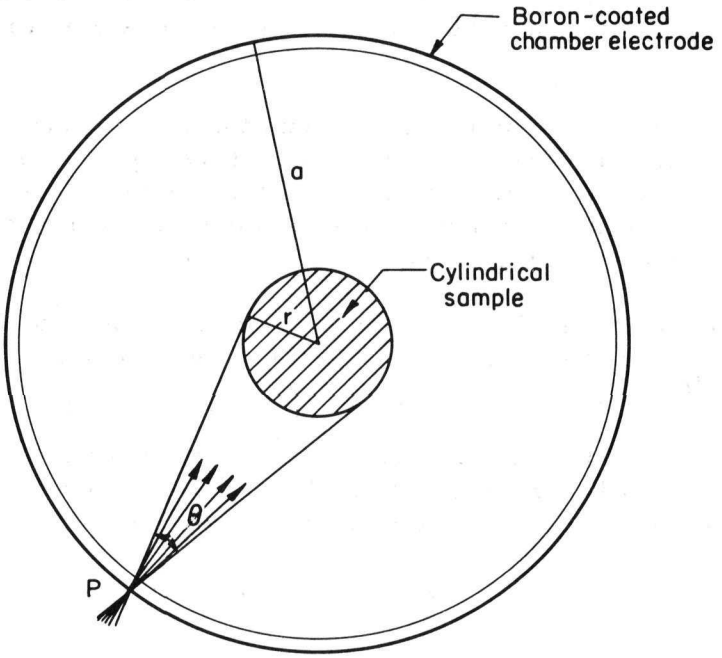

a. Geometry for Cylindrical Samples

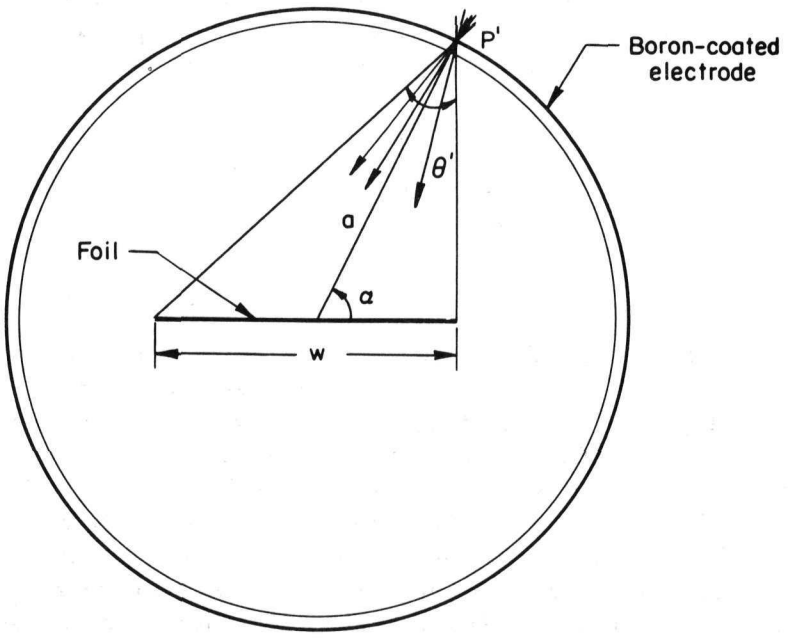

b. Geometry for Foils

FIGURE 19. GEOMETRY OF SAMPLES AND ION CHAMBER

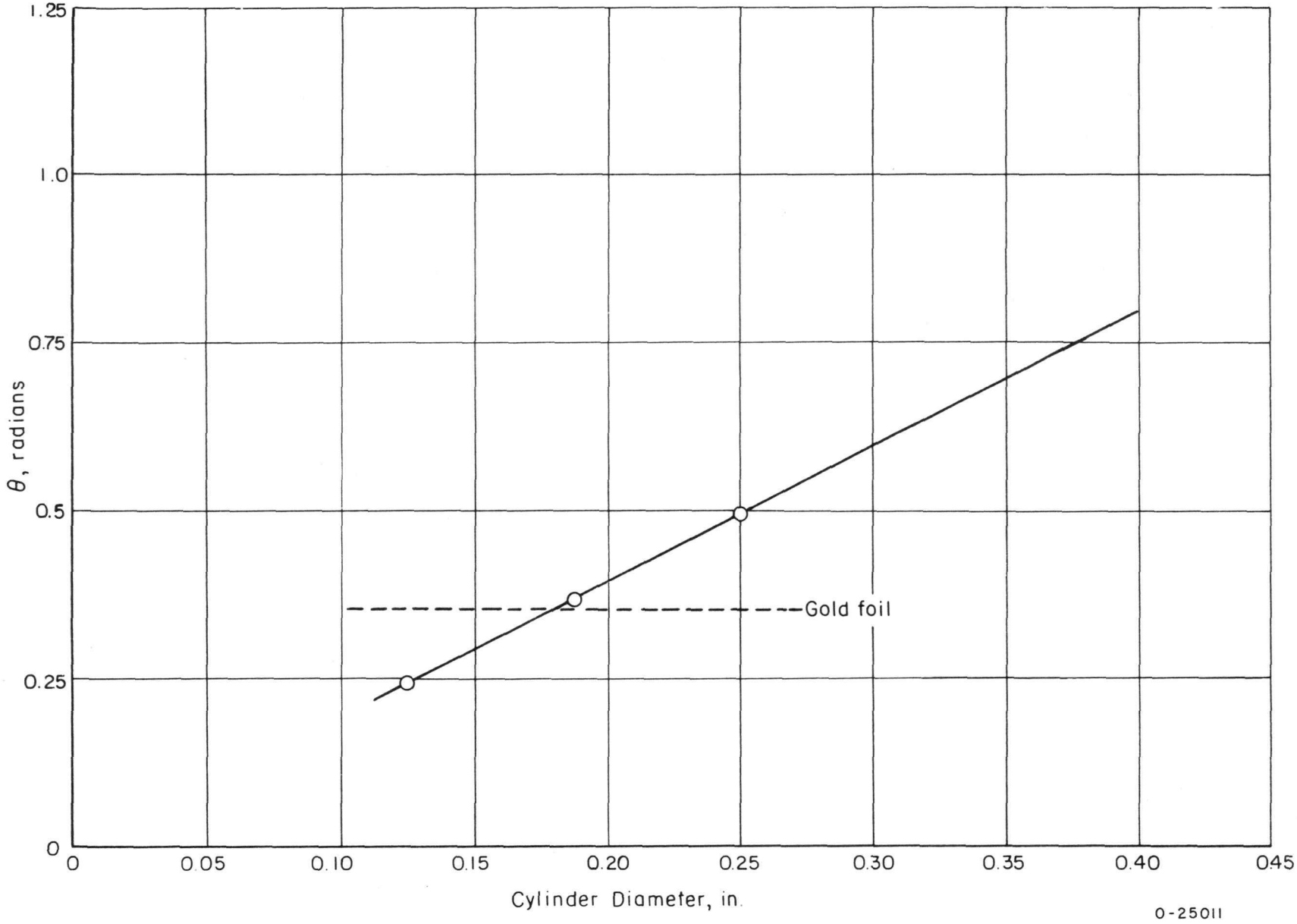

FIGURE 20. VARIATION OF ANGLE θ WITH CYLINDER DIAMETER

TABLE 5. PREPARATION OF POWDERED-METAL SAMPLES

Material	Weight, g	Compacting Pressure, psi	Heat Treatment	Remarks
Niobium	15.562	60,000	Sintering conducted at 2150 C for 3 hr under a vacuum of 0.035 μ	Density after sintering 7.31 g per cm^3, or 85.3 per cent of theoretical density
Iron	9.670	30,000	Sintered for 1-1/6 hr at 2000 F in hydrogen atmosphere	Allowed to cool to approximately 100 F in the hydrogen atmosphere
Nickel	11.735	30,000	Sintered for 1-1/4 hr at 1850 F in hydrogen atmosphere	Allowed to cool to approximately 100 F in the hydrogen atmosphere

The observed variation of measured cross sections with geometry emphasizes the importance of matching the geometry of the unknown sample to that of the standard.

CROSS-SECTION MEASUREMENTS

The principal cross sections which have been measured to date (other than those measured in the calibration and geometry studies) are those for powdered metals. The powder material for these samples was compacted at Battelle. A special die was prepared to form the sample into the shape of rectangular bars, 3/16 by 5/16 by 2 in. The powders and their treatment are given in Table 5.

The cross sections of the powdered-metal samples were measured using the iron sample as the standard, since its cross section is known to better accuracy than the other samples. These values are compared with cross-section measurements obtained at the ORNL oscillator in Table 6.

TABLE 6. COMPARISON OF THE CROSS SECTIONS OF THE POWDERED-METAL SAMPLES

Sample	Cross Section, mm^2 per g		Probable Error of Battelle Measurement
	ORNL Value	Battelle Value	
Iron	2.65	2.73[a]	±0.04[a]
Niobium	0.86	0.725	±0.05[b]
Nickel	4.00	4.09	±0.08[b]

(a) Assumes BNL-325 cross-section value for standarization.
(b) Total probable error. Includes error from standard and probable error in integrator readings.

As seen from this table, agreement between the iron and nickel samples is good, but the niobium measurements disagree. However, the Battelle value yields a microscopic thermal-neutron-absorption cross section of 1.12 ± 0.11* barns, which compares favorably with the value of 1.1 ± 0.1 barns reported in BNL-325. The error of the measurement, while similar to the BNL-325 value, could be further reduced with a better standard.

DISCUSSION OF ERRORS

Variations occur in the amplitude of the signal generated by the neutron-absorbing sample in passing through the ion chamber due both to small variations in reactor power level (reactor "noise") and to ion-chamber noise. Good statistics are obtained in the measurements by oscillating the sample through the ion chamber many times. In practice, the chamber pulses are integrated and at the conclusion of a predetermined number of oscillations the accumulated signal is read from a d-c microammeter. The number of oscillations required to obtain good statistics is determined empirically, and, generally, the smaller the total absorption cross section being measured, the larger the number of oscillations required. For cross sections greater than about 10 mm^2, approximately 40 oscillations (corresponding to a 1-min integration) have been found to yield accurate results. For cross sections less than 10 mm^2 the number of oscillations per reading is increased.

For the sake of assigning a probable error to the integrator reading, five or more runs are usually made with each sample and the probable error determined from the relationship

$$S_{\bar{I}} = 0.6745\sqrt{\frac{\sum_{i=1}^{n}(\Delta X_i)^2}{n(n-1)}}\ , \qquad (8)$$

*Standard deviation instead of probable error, for the sake of comparison.

where

$S_{\bar{I}}$ = probable error associated with the average of the integrator readings

ΔX_i = deviation of the ith reading from the average reading

n = number of readings.

The constancy of the integrator readings is shown by the small probable error assigned to the integrator readings given in Table 2. As seen from the values in this table, the error introduced by the integrator reading is generally 1 per cent or less.

A possible source of error in obtaining the actual thermal-neutron-absorption cross section from the integrator reading is the contribution to the absorption signal from absorption of resonance neutrons by the sample. Table 7 lists the thermal-neutron-absorption cross sections and resonance-absorption integrals for the more common structural materials and impurities commonly occurring in these materials[9].

TABLE 7. THERMAL-NEUTRON-ABSORPTION CROSS SECTIONS AND RESONANCE-ABSORPTION INTEGRALS FOR COMMON REACTOR STRUCTURAL MATERIALS AND IMPURITIES OCCURRING IN THESE MATERIALS

Element	Microscopic Thermal-Neutron-Absorption Cross Section, barns	Resonance-Absorption Integral, barns	Ratio of Resonance-Absorption Integral to Thermal-Absorption Cross Section
Lithium	71	28	0.39
Sodium	0.515	0.27	0.52
Magnesium	0.063	0.9	14
Aluminum	0.230	0.18	0.78
Silicon	0.13	0.5	0.38
Phosphorus	0.20	2	10
Sulfur	0.49	0.6	1.2
Chlorine	32.6	12	0.37
Potassium	1.97	1.1	0.56
Calcium	0.43	2	4.6
Chromium	2.9	1.9	0.65
Manganese	13.2	10.8	0.82
Iron	2.53	2.3	0.91
Cobalt	37.0	48	1.3
Nickel	4.6	4	0.87
Copper	3.69	4	1.1
Zinc	1.06	2	1.9
Zirconium	0.180	3	17

For the light elements such as sodium and aluminum, the absorption cross section in the resonance energy range is approximately 1/v and the resonance-absorption integral is about one-half the thermal-absorption cross section[2]. Notable exceptions are magnesium and phosphorus. With the previously derived ratio of thermal-to-total resonance-neutron flux of at least 320, resonance absorption for the light elements with 1/v cross-section behavior would contribute only about 1 part in 640 to the integrator reading. The next group of elements above the light-element group exhibits several resonances and have resonance-absorption integrals approximately equal to the thermal-absorption cross section. Cobalt, copper, iron, manganese, and nickel are representative of this group. For these elements the resonance absorption still contributes only 1 part in several hundred to the integrator reading. When the elements occur as impurities (as is common) in other materials, appearing in quantities of several per cent at the most, the resonance-absorption effect is completely negligible. For many of the heavy elements the cross section exhibits more numerous and higher resonance peaks and the resonance-absorption integral may be 10 to 100 times larger than the thermal-absorption cross section. Individual analysis of possible error due to resonance absorption by these elements must be performed for each sample of materials in this group. However, if it is only impurities of materials in this group which are present, the resonance-absorption effect will still be negligible.

In order to prevent errors from being introduced by self-protection effects, it is necessary that the total absorption cross section of the sample be less than 40 to 45 mm^2. At this cross-section region it has been observed that self-protection effects become significant for both foils and large samples.

With the present instrumentation, error in the true absorption signal due to amplifier overloading is prevented by restricting the upper limit of total absorption cross sections to those values shown in Table 8. Each of these values corresponds to an output voltage of approximately 68 v.

TABLE 8. LIMITS OF TOTAL ABSORPTION CROSS SECTION ON THE VARIOUS AMPLIFIER GAINS DUE TO AMPLIFIER OVERLOADING

Amplifier Gain	Upper Limit of Total Absorption Cross Section, mm^2
1	75
2	55
3	38
4	26
5	18

Appreciable error can be introduced by differences in geometry between the standard and the unknown sample. Foils, in general, make improper standards for the large slab or cylindrical samples. For example, from the geometry study discussed previously, a difference of about 8.5 per cent exists in the integrator reading between a gold foil having a total absorption cross section of about 32 mm^2 and a copper slab (0.100 in. in width) having the same cross section. If the geometry of the samples is similar but with slight variations in the dimensions, significant errors can also be introduced. For example, from Figure 18 it can be seen that, for cylinders of diameter on the order of 1/8 in., a difference of 0.01 in. between the diameter of the standard and unknown sample would introduce an error of about 8 per cent in the observed cross section, i.e., if the mass of the samples had been determined and the diameters assumed to be identical, the cross section deduced from comparison of the integrator readings produced by oscillation of the known and unknown sample would be in error by 8 per cent. For this reason a careful dimensional check must be made on all samples. Compressed powdered-metal samples are produced from the same die to eliminate this source of error.

The principal limit to the accuracy of cross-section data obtained by the comparison technique of the pile oscillator is the absolute accuracy to which the cross section of the standard is known. The cross section of gold, although as yet not completely resolved, has been generally accepted to be 98.0 ± 1.0 barns[1]. Thus, the limiting accuracy of the oscillator technique is at present about 1 per cent. Substandards can be prepared in special geometries from the gold standard to accuracies of about 2 per cent.

Generally, a knowledge of the absorption cross section in terms of mm^2 per g of material is sufficient for engineering applications. Examination of Equation (5) reveals that in order to obtain the cross section of an unknown material in terms of mm^2 per g, it is necessary only to know the weight of the sample and its total cross section deduced from comparison with the standard. Thus, the formula for obtaining the cross section of an unknown in terms of mm^2 per g is

$$\sigma_u\left(\frac{mm^2}{gram}\right)=\left(\frac{M_o}{M_u}\right)\left(\frac{I_u}{I_o}\right)\sigma_o \quad , \tag{9}$$

where

σ_u = total thermal-neutron-absorption cross section of unknown sample, mm^2 per g

σ_o = total thermal-neutron-absorption cross section of standard, mm^2 per g

M_u = mass of unknown sample, g

M_o = mass of standard sample, g

I_u = integrator reading produced by unknown sample for a given number of oscillations on a given amplifier gain

I_o = integrator reading produced by standard sample for the same number of oscillations on the same gain as for the unknown.

Precision in measurement of the weights of the samples is easily attained with a standard analytical balance, and, in general, error from this source is of no consequence. Assuming negligible error from the weight determinations, identical sample geometry, and no resonance-absorption effects (these errors can be included if determined to be significant), the probable error associated with the determination of σ_u in Equation (9) is given as

$$S_{\sigma_u} = \left[\left(\frac{\partial \sigma_u}{\partial I_u} \right)^2 \left(S_{\bar{I}_u} \right)^2 + \left(\frac{\partial \sigma_u}{\partial I_o} \right)^2 \left(S_{\bar{I}_o} \right)^2 + \left(\frac{\partial \sigma_u}{\partial \sigma_o} \right)^2 \left(S_{\sigma_o} \right)^2 \right]^{1/2} , \qquad (10)$$

where

S_{σ_u} = probable error in σ_u determination

$S_{\bar{I}_u}$ = probable error associated with the average value of the integrator readings of the unknown sample

$S_{\bar{I}_o}$ = probable error associated with the average value of the integrator readings of the standard sample

S_{σ_o} = probable error in σ_o of the standard.

S_{σ_o} is known and $S_{\bar{I}_u}$ and $S_{\bar{I}_o}$ are determined from Equation (8).

In order to deduce the microscopic absorption cross section, the atomic weight of the material must be known. High purity of the material or accurate analysis of the impurities must be assured in assigning the value of the atomic weight. Generally, reduction of the data to obtain the microscopic absorption cross section is unnecessary.

From the sources of errors which have been discussed, it is apparent that with very special precautions (such as exact duplication of geometry between the known and unknown samples) accuracies of cross sections may be measured to within several per cent. Measurements to these accuracies can be accomplished, of course, only on samples which have total absorption cross sections within the present range of sensitivity of the apparatus. The range of sensitivity of the apparatus is not precisely defined, but with the present system total absorption cross sections greater than about 1 mm^2 can be determined with precision. At cross sections much smaller than 1 mm^2, the presence of reactor and instrument noise masks the absorption signal to the extent that many oscillations are required to obtain reasonable statistics on the data. With some modifications the noise sources can be reduced to increase the sensitivity of the oscillator. However, for the materials of current interest the present sensitivity is sufficient.

CONCLUSIONS

As a result of the development and testing of the modified pile oscillator it is concluded that:

(1) An apparatus has been developed to measure total thermal-neutron-absorption cross sections in the range of 1 to 45 mm^2 to accuracies within ±5 per cent.

(2) Geometry differences in the samples being measured can introduce significant differences in the apparent cross sections.

(3) With the continuous graphite-rod sample carrier appreciable scattering effects are eliminated, and for the samples studied the effects of neutron scattering were not significant.

(4) The ratio of thermal neutrons to resonance neutrons in the vicinity of the pile oscillator is sufficiently large to eliminate corrections on the cross-section data for resonance absorption for most samples of present interest.

REFERENCES

(1) Hughes, D. J., and Harvey, J. A., "Neutron Cross Sections", BNL-325 (July 1, 1955).

(2) Hughes, D. J., Pile Neutron Research (1953).

(3) Weinberg, A. M., and Schweinler, H. C., Phy. Rev., 74, 851 (1948).

(4) Hoover, J. I., Jordan, W. H., Moak, C. D., Pardue, L., Pomerance, H., Strong, J. D., and Wollan, E. O., "Measurement of Neutron Absorption Cross Sections With a Pile Oscillator", Phy. Rev., 74, 864 (1948).

(5) Langsdorf, A., "The Thermal Neutron Reactor as an Instrument for Measuring Neutron Cross Sections", AECD-3194 (February, 1950).

(6) Greenfield, M. A., "Measuring the Ratio of Thermal to Resonance Neutron Densities Using Thick Indium Foils", Nuclear Science and Engineering, 2 (1957).

(7) Kunstadter, J. K., "A Correction to Be Applied to the Activity of Neutron-Activated Cadmium-Covered Indium Foils", Phy. Rev., 78, 484 (1950).

(8) Small, V. G., and Sturway, A. H., "Oscillator Apparatus for the Measurement of Thermal-Neutron Absorption Cross Sections in B.E.P.O.", AERE-RP/R-1439.

(9) Nucleonics, Data Sheet No. 23 (March, 1958).

JNA:RGJ:JWC/bjw